

**Asymmetry in the Planform Morphology of Alluvial Fans:  
A Geomorphological Analysis**

By

Bryce Matthew Whitehouse

A Thesis Submitted to  
Saint Mary`s University, Halifax, Nova Scotia  
In Partial Fulfillment of the Requirements for  
The Degree of Bachelor of Science Geography (Honours)

April, 2013, Halifax, Nova Scotia

© B.M. Whitehouse, 2013

Approved: Dr. Philip T. Giles  
Supervisor

Approved: Dr. Robert J. McCalla  
Reader

Date: April 11, 2013

## **ABSTRACT**

### **Asymmetry in the Planform Morphology of Alluvial Fans:**

#### **A Geomorphological Analysis**

By Bryce Matthew Whitehouse

Since alluvial fans became a topic of modern research in the 1960's, there has been a lack of research publications on fan asymmetry in planform. The aim of this study is to provide some insight into the planform morphology of fans being modified by axial rivers. Fans chosen for this study had to be in areas with adequate accommodation space, and could not be encroached upon by other fans nor have conjoining valleys near the apex. The broad glaciated valleys of Yukon, Canada, and Alaska, U.S.A, contain a sufficient number of suitable fans to build a dataset for planform asymmetry analysis. To collect these data, individual fans were outlined in Google Earth and divided geometrically into five equal "pie" parts. Profiles along outer parts of the fan were then measured in length from apex to toe, with the ratio of longer to shorter profile representing the degree of fan asymmetry. Results show that fans modified by axial rivers do predominantly have longer profiles on the downstream side of the axial valley, meaning that the planform morphology is asymmetrical. In addition to planform asymmetry, this study will investigate whether there is a significant difference in longitudinal profile gradients between the upstream and downstream side on asymmetrical fans, and whether the distribution of fan surface streams is affected by fan asymmetry.

April 11, 2013

## RÉSUMÉ

Depuis que les éventails alluvionnaires sont devenus un sujet moderne de recherche dans les années 1960s, il y a un manque de recherche publié concernant l'asymétrie d'éventails. Le but de cette recherche est de fournir un aperçu de morphologie d'éventails vus d'en haut qui sont modifiés par des rivières axiales. Les éventails choisis pour cette étude devaient être dans une zone avec un espace adéquat, qui ne pouvaient pas être empiétés par d'autres éventails, et qui n'avaient pas de vallées conjointes près du point culminant. Les vallées vastes dans le Yukon, Canada, et dans l'Alaska, é-U, contiennent un nombre suffisant d'éventails pour créer une base de données pour une analyse asymétrique. Afin de recueillir ces données, des éventails individuels ont été tracés à partir de Google Earth et divisés géométriquement en cinq secteurs. Les profils le long de l'extérieur des éventails mesurés en longueur depuis le point culminant jusqu'au pied, le ratio entre le plus long profil et plus court profil représentant le degré d'asymétrie de l'éventail. Les résultats montrent que les éventails modifiés par des rivières axiales ont majoritairement de plus longs profils du côté en aval de la vallée axiale, signifiant que la morphologie est asymétrique. En plus de l'asymétrie, cette étude enquête s'il y a une différence importante en aval et en amont dans le gradient de longs profils d'éventails asymétriques et si la distribution de ruisseaux en surface de l'éventail est affecté par l'asymétrie d'éventails.

**Asymmetry in the Planform Morphology of Alluvial Fans:  
A Geomorphological Analysis**

By

Bryce Matthew Whitehouse

A Thesis Submitted to  
Saint Mary's University, Halifax, Nova Scotia  
in Partial Fulfillment of the Requirements for the  
Degree of Bachelor of Science in Geography (Honours)

April, 2013, Halifax, Nova Scotia

© B.M. Whitehouse, 2013

Approved: \_\_\_\_\_  
Dr. Philip T. Giles  
Supervisor

Approved: \_\_\_\_\_  
Dr. Robert J. McCalla  
Reader

Date: \_\_\_\_\_

## **ACKNOWLEDGEMENTS**

First the supervision and the guidance provide by Dr. Philip Giles is greatly acknowledged. Second the secondary reader of this thesis Dr. Robert McCalla and my fellow students and friends that provided me with helpful feedback and comments, Sarah Manchon for the translation of the abstract. Finally my mother Sally Whitehouse, and my father Bruce Whitehouse; if it were not for their wisdom and support this project would not have been possible.

Halifax, Nova Scotia  
April, 2013

## TABLE OF CONTENTS

|  |     |
|--|-----|
| Approval Page .....                                | ii  |
| Abstract .....                                     | iii |
| Résumé.....  | iv  |
| Acknowledgements .....                             | v   |
| <br>   |     |
| List of Tables .....                               | iii |
| List of Figures .....                              | ix  |
| List of Equations .....                            | xi  |
| <br>   |     |
| Chapter 1: Introduction and Literature Review..... | 1   |
| Chapter 2: Study Areas .....                       | 19  |
| Chapter 3: Methods.....                            | 34  |

|   |    |
|---|----|
| Chapter 4: Alluvial Fan Asymmetry: Results and Discussion .....           | 43 |
| Chapter 5: Gradient and Stream Distribution: Results and Discussion ..... | 51 |
| Chapter 6: Cumulative Discussion and Conclusions.....                     | 63 |
| Reference List.....   | 70 |
| Appendix .....  | 75 |

## LIST OF TABLES

|   |    |
|---|----|
| Table 1: Asymmetry Index one tailed hypothesis test breakdown.....      | 47 |
| Table 2: Gradient Difference two tailed hypothesis test breakdown ..... | 57 |
| Table 3: Stream distribution two tailed hypothesis test breakdown ..... | 61 |
| Table A1: Collected alluvial fan data .....                             | 76 |
| Table A2: Calculated fan gradient and gradient difference .....         | 80 |
| Table A3: Calculated valley gradient.....                               | 82 |



## LIST OF FIGURES

|   |    |
|---|----|
| Figure 1: Diagram of an alluvial fan .....                                      | 4  |
| Figure 2: Detailed map of upper Kaskawulsh Valley alluvial fans.....            | 20 |
| Figure 3: Slims and Kaskawulsh Valleys study areas .....                        | 23 |
| Figure 4: Dusty and Alsek Valleys study areas.....                              | 24 |
| Figure 5: Small scale western Kaskawulsh Valleys study area .....               | 25 |
| Figure 6: Donjek Valley study area .....  | 26 |
| Figure 7: West Robertson and Robertson Valleys study areas.....                 | 28 |
| Figure 8: Chilligan Valley study area .....                                     | 29 |
| Figure 9: Styx and Skwentna Valleys study areas .....                           | 30 |
| Figure 10: Copper and West Chitina Valleys study areas .....                    | 31 |
| Figure 11: Eastern Chitina Valleys study area .....                             | 32 |
| Figure 12: An example of an outlined alluvial fan in Google Earth.....          | 36 |
| Figure 13: Data collection layout outlined alluvial with edge lines added ..... | 37 |
| Figure 14: Data collection layout sectors added.....                            | 38 |
| Figure 15: Data collection layout mid lines added to outer sectors.....         | 39 |
| Figure 16: Finished data collection layout imported into Google Earth.....      | 40 |
| Figure 17: Asymmetry Index distribution histogram.....                          | 44 |
| Figure 18: Valley gradient side profile.....                                    | 46 |

|  |    |
|--|----|
| Figure 19: Asymmetry Index hypothesis test results under a normal curve .....            | 48 |
| Figure 20: False fan gradient profile .....  | 53 |
| Figure 21: Gradient paired difference histogram.....                                     | 55 |
| Figure 22: Gradient paired difference hypothesis test results under a normal curve ..... | 57 |
| Figure 23: Stream distribution histogram .....   | 59 |
| Figure 24: Stream distribution hypothesis test results under a normal curve .....        | 61 |
| Figure 25: Initial asymmetrical fan development .....                                    | 64 |
| Figure 26: Steady state fan asymmetry.....   | 67 |

## LIST OF EQUATIONS

|  |    |
|--|----|
| Equation 1: Asymmetry index calculation .....  | 43 |
| Equation 2: Z-score equation for one-tailed hypothesis test .....                    | 44 |
| Equation 3: Difference in valley elevation.....                                      | 49 |
| Equation 4: Valley gradient calculation.....   | 49 |
| Equation 5: Upstream gradient calculation .....                                      | 51 |
| Equation 6: Downstream gradient calculation.....                                     | 51 |
| Equation 7: t-score statistic for two-tailed paired difference hypothesis test.....  | 54 |
| Equation 8: Z-score test for two-tailed hypothesis test of stream distribution ..... | 58 |

## CHAPTER 1

### INTRODUCTION AND LITERATURE REVIEW

#### 1.1 Introduction to Study

When it comes to alluvial fan research, fan morphology has been a topic that has received much attention within the field of geomorphology. Fan morphology has been studied from multiple perspectives within various regions. Alluvial fans can be found in all climatic regions on Earth, although regions with mountainous catchments that drain into lowland areas have the greatest potential for alluvial fan development. At first glance alluvial fans from different regions may appear to be the same, but upon further investigation one would see that alluvial fan development and morphology is greatly influenced by the natural processes of the region in which they exist.

Alluvial fans are depositional landforms which are easily recognizable in air photographs and satellite imagery. Some larger fans are more easily spotted from aerial imagery than they are from the ground because their change in elevation over distance is so gradual that a fan can be mistaken for another topographic feature. The aerial imagery or planform view provides an interesting perspective for researchers studying alluvial fans, as in a planform perspective it is possible to gather elevation and distance data through various sources such as topographic maps, satellite imagery and aerial photographs. When viewing alluvial fans from this perspective the shape of a fan stands out above all other characteristics. Alluvial fans shape can vary; Blair and McPherson

(2009) described them as semi-conical depositional landforms, but this description can give one a limited impression of the variety of shapes an alluvial fan can take. Harvey (2011) mentioned that alluvial fans are conical landforms that are modified by whatever confinement may be present. Harvey's definition of an alluvial fan is similar to Blair and McPherson's but it takes into account that fans do not always have perfectly conical shapes. Expanding on Harvey's definition, alluvial fan morphometry can also be modified by secondary processes such as overland flow, wind erosion, weathering and lateral erosion (Bull 1977; Harvey 2011). Lateral erosion is the wearing away of the toe of an alluvial fan by an axial river (Leeder and Mack 2001); Lateral erosion can cause the shape of an alluvial fan to change and be asymmetrical in planform.

Asymmetrical morphology of alluvial fans, or even the idea of fan asymmetry, has received little attention in published research. As suggested by Harvey (2002), interactions between alluvial fans and non-fan features are essential to better understand the characteristics of alluvial fans. In this study the effects of the interaction between alluvial fans and axial rivers is investigated. More specifically, this study investigates: 1) asymmetry of alluvial fans in planform morphology: 2) if there is a difference (or lack thereof) fan gradient between two distance profiles on the upstream and downstream side of a fan: 3) the distribution of surface on the fan surface by using freely available data (imagery from Google Earth, topographic maps from Natural Resources Canada, and United States Geological Survey). A unique methodology (described in Chapter 3) is used that incorporates an original data collection layout to collect relevant data.

### **1.1.2 Definition of Fan Asymmetry**

Asymmetry of alluvial fans can be perceived in a few different ways, for example, volume of sediment, or area. This study specifically defines alluvial fan asymmetry as a significant difference in length from apex to toe between the upstream side and the downstream side of an alluvial fan. Asymmetry in this study is viewed in planform and is analyzed in planform. As mentioned later fan asymmetry has not been analyzed directly in research so this analytical technique is a new idea. For convenience purposes the way alluvial fan asymmetry is perceived in this study will be referred to as 'the idea of alluvial fan asymmetry.'

## **1.2 Definition and General Morphology of Alluvial Fans**

In the traditional or classic sense, an alluvial fan is a semi-conical depositional landform that typically develops where a confined stream channel emerges from a mountainous catchment into an adjoining broad valley or lowland area (Harvey 2011; Blair and McPherson 2009) illustrated in Figure 1. The highest point of an alluvial fan, the apex, is the point where a channel emerges from the mountain catchment. Beyond the apex is the surface the part of the fan which dips away from the mountain catchment and said apex (Harvey 2011). Radiating channels cut into the face of the fan are the deepest at the apex and become less so with increasing distance eventually converging with the surface. These radiating channels build up the face and the fan shape characteristic gradually as the stream shifts back and forth across the fan's

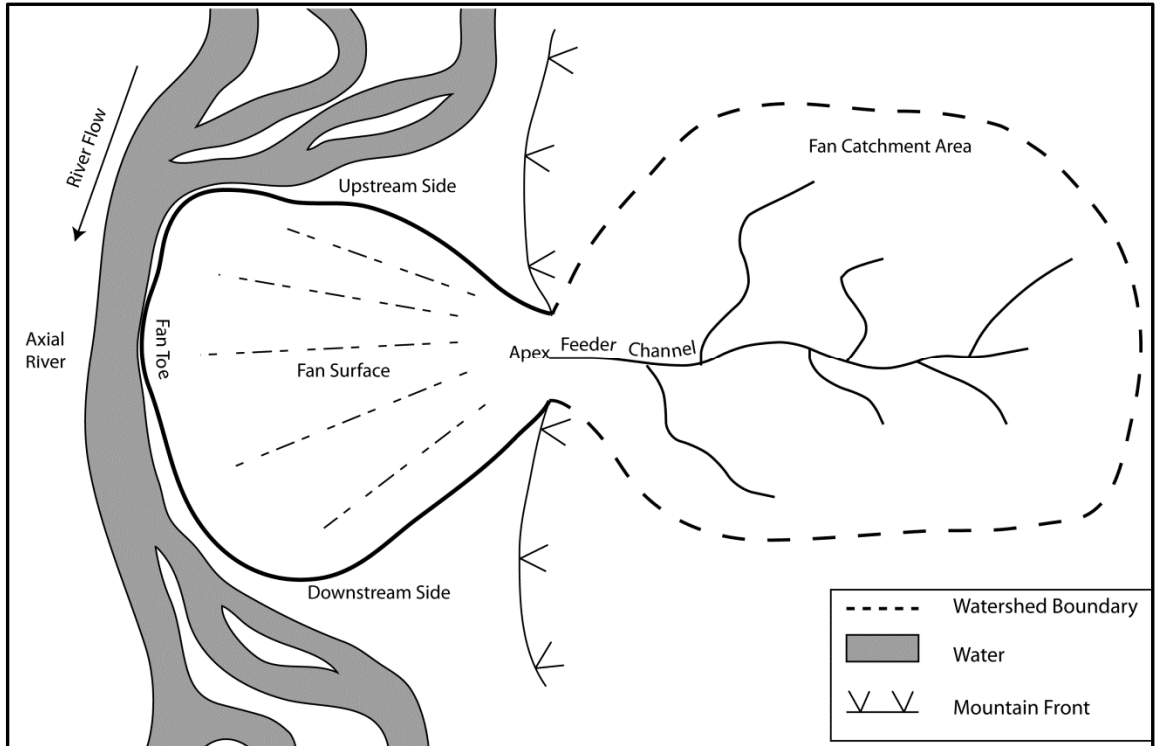


**Figure 1.** A diagram of an alluvial fan in planform within a glaciated valley, with an axial river present

surface in a braided pattern (Plummer *et. al.*, 2007).

The lower boundary of the fan where the face meets an area of flat land or low gradient is called the fan toe or boundary, but here forth will be referred to as the fan toe (Huggett 2011). The ruggedness of the surface of alluvial fans can range from a large block of angular clasts to a sandy-silt surface and everywhere in between. Vegetation is common on fans and can vary from sparse cacti and other xerophytes in arid regions to more dense grasses shrubs and trees in alpine regions.

Alluvial fans can range greatly in size (lengths from apex to toe) from hundreds of metres to tens of kilometers. Some fans, for example in Queensland, Australia, are easy to see on topographic maps and satellite images, but are not recognizable on the ground because the radius is around one hundred kilometers (Huggett 2011). Since there is a point where the definition of an alluvial fan and a floodplain is ambiguous it can be debated that an alluvial fan with a radius close to 100 kilometres could be defined instead as a floodplain (Huggett 2011; Saito and Oguchi 2005). The exact definition of an alluvial fan can be argued in very extreme cases, like the fans in Queensland. Oguchi (2005) mentioned that surface gradient is a defining factor when trying to distinguish an alluvial fan from a floodplain and a talus slope; a low gradient alluvial fan that terminates in standing water is referred to as a delta, or a fan that has very low gradient ( $< 1^\circ$ ) over a very large distance ( $> 5$  km) can be called floodplain, whereas a steep fan ( $> 5^\circ$ ) is defined as a talus slope (Saito and Oguchi 2005). Saito and Oguchi (2005) state that an alluvial fan is a conical depositional landform that has a slope between  $1^\circ$  and  $5^\circ$ , and doesn't terminate in a water body. Depositional features with less than  $1^\circ$  are typically defined as a floodplain, and anything greater than  $5^\circ$  is defined as a talus slope (Saito and Oguchi 2005). In contrast, this study has found some examples of alluvial fans that have surfaces with gradients greater than  $5^\circ$ . These findings go to show that there are still some ambiguities between talus slopes, floodplains and alluvial fans.

Alluvial fans tend to be more complex longer term features than debris cones or tributary junction fluvial fans, often dating back to the late Pleistocene (Harvey 2010). Local controls on alluvial fans are those of long term geomorphological evolution.



Examples of these controls are tectonics or glaciation, creating the juxtaposition of sediment source area, and accommodation space. These local controls make alluvial fans dynamic landforms. Their formation may be modified by whatever confinement is in the adjacent area and by external environmental forces like climate change, tectonic movements, base level change and internal feedbacks between processes and form (Nicholas *et al.* 2009).

The gradient is a morphology variable of a fan dependent on the style of deposition, clast size, and stream power, with the steepest alluvial fans being associated with the smallest streams and coarsest load (Bull 1979; Harvey 2010). On larger fans sediment is graded in size with the coarser grained sediment is deposited near the apex and the finer grained sediment being dropped out of suspension progressively further away (Plummer 2007; Blair and McPherson 2009). For sediment to accumulate and eventually form an alluvial fan there must be accommodation space for the material carried by the feeder channel to be deposited where the stream power is reduced (Viseras *et. al.*, 2003). Accommodation space is defined by Posamentier and Vail (1988) as space made available for potential sediment to fill between the old stream profile and a new higher stream profile. The threshold of critical stream power is fundamental to fan development, since alluvial fans are sensitive to this threshold changing (Bull 1979; Wells and Harvey 1987; Harvey 2010). If there is a change in the water-to-sediment ratio, the transport and depositional processes may switch between debris flows and fluvial processes (Harvey 2010). According to Miall (1996), rivers and fans adjust to changes in base level whether the change is from tectonic movements or hydraulic conditions.

In this study accommodation space has been provided as a result of glaciers receding and leaving behind wide, low gradient parabolic-shaped valleys. Adjoining feeder channels that were once blocked by ice are now for the most part unimpeded with their mouths at a higher elevation than that of the valley below. This difference in elevation creates new accommodation space, which happens when the graded profile moves upwards (or in this case removal of a blockage) in a response to base level change (Harvey 1984, 1987).

### **1.3 Occurrence of Alluvial Fans Globally**

Alluvial fans have been described in various environments, including Arctic environments (Ritter and Ten Brink 1986), alpine environments (Derbyshire and Owen, 1990), humid temperate regions (Chiverrell, Harvey and Foster 2007) and even in humid tropics (Kesel and Spicer 1985). Conditions that favour alluvial fan development are in arid and semi-arid mountainous regions, because of the availability of loose surface sediment that is easily entrained by overland flow (Harvey 2011). Alluvial fans are particularly well developed and exposed in the south-western deserts of the United States and in other semi-arid regions like southern Europe and the Canadian Arctic (Ritter and Ten Brink 1986; Plummer 2007; Harvey 2011).

Most research literature has focused on fans from the south-western United States, but since the 1970's research literature has emerged that describes fans in other regions as well. Apart from the studies done in the United States, the majority of alluvial

fan research since the 1970's has been based on fans in the Mediterranean regions of Europe. There has been a range of studies done on fans in the semi-arid regions of Spain and Italy dealing with fan sediments (Gomez-Villar and Ruiz, 2000), morphological sequences and morphometry (Calvache *et. al.*, 1997). More recently, a study from Europe have focused on fan evolution and dynamics in relation to tectonic, climatic and base level change (Viseras 2003). Only until recently has research focused on fans from South America, in the Atacama Desert (for example, Huag *et. al.*, 2010) and in the Argentinian Andes (Sancho *et. al.*, 2008). In Australia, Gardener *et. al.* (2006) have described fan deposition at Cape Liptrap, and Williams (1973) has described morphology in the Flinders Range and elsewhere. Asia has limited primary research compared to the other regions mentioned, but they do have alluvial fan research on large fans in the Taklimakand Desert in northwest China (Harvey 2011). Also, there have been studies that cover multiple Asian countries such as Saito and Oguchi's (2005) article concerning slopes of alluvial fans in Japan, Taiwan and the Philippines. In India there has been research focused particularly on 'megafans' first described by Gohain and Parkesh (1990) and recently by Chakarabarty and Ghosh (2005). In Canada and Alaska the majority of fan studies have focused on fan morphology in the Quaternary, particularly since the last ice age (e.g. Campbell 1998; Levson and Rutter 2000; Beaudoin and King 1994).

#### **1.4 Geomorphological Development of Alluvial Fans**

Fan morphology depends on the nature of the processes transporting sediment to the fan and on the mechanisms of deposition. Sediment transport may include a

variety of debris-flow processes (Blair and McPherson 1994) and tractional processes in water flow that can range from unconfined sheetflows to channelized fluvial processes (Harvey 2010). Alluvial fans can also have a range of stream patterns present on the surface; these channels may be braided, meandering or anastomosing (Gabris and Nagy 2005).

Conditions necessary for optimal fan development are: (a) a topographic setting where an upland catchment drains into a valley, (b) sufficient sediment production in the catchment to build the fan, (c) sparse vegetation, (d) supply of water from rainfall or glacier melt, and (e) a trigger mechanism, usually sporadic high periods of high water discharge or, less commonly tectonic movement (Laronne and Reid 2002; Blair and McPherson 2004). Common topographic settings for fans are marginal to uplifted structural blocks bounded by faults (Blair and McPherson 2004), where tributary channels enter a canyon or valley (Florsheim 2004), or where there is bedrock exposure possessing relief by differential erosion (Harvey 1990).

The sediment required for the development of alluvial fans is typically met given time, because of the presence of relief and because of the continuous weathering of rocks. Areas with high topographic relief promote fan development; the relief provides the high potential energy required for streams and rivers to transport high quantities of sediment. Sediment yields increase exponentially with relief due to the effect of gravity on slope erosion (Schumm 1963, 1977; Ahner 1970). In arid to semi-arid environments the weathering processes such as fracturing, exfoliation, root wedging, hydrolysis, dissolution and oxidation produce most sediments carried to alluvial fans. Weathering

processes are greatly promoted along structurally controlled mountain fronts because of tectonic fracturing which exposes significantly more rock to alteration than in unfractured rocks (Plummer *et. al.*, 2007).

Non-tectonically active regions have little to no fracturing exposing new rock so weathering occurs, but at a much slower rate than in tectonically active regions. Seismic activity may be one process that produces sediment for alluvial fan development, but it is not necessary for development. Alluvial fans can develop in paraglacial environments where there is below average seismic activity exposing little amounts of new rock; but, in these environments with little seismic activity, the retreat of a glacier could have deposited much of the sediment needed for fan development in the form of moraines (Blair and McPherson 2009). Therefore, the development of a fan in paraglacial environments may be fast because of the high sediment yield after a glaciation event, but once the initial source of sediment (moraines) feeding a certain fan has been exhausted, sediment deposition on alluvial fans decrease rapidly.

The key processes that achieve sediment transport are related to water input and the freeing up of sediment by means of mass wasting (Blair and McPherson 2004). These processes are promoted by heavy or prolonged rainfall, rapid ice melt and snowmelt, or the rapid release of a natural reservoir (Huggett 2011). Precipitation that falls in mountainous regions is directed through a series of short stream segments to the main feeder channel. Mass wasting events provide high volumes of poorly sorted sediment to the feeder channel which rapidly increases the sediment discharge of the catchment and can even create new first order streams (Patton 1988). A combination of

mass wasting events and fluvial processes transport the sediment to alluvial fans via a feeder channel. Sediment is deposited where there is a reduction of stream power or gradient (for example, at the mouth of a drainage basin emptying into a larger parabolic valley that can contain a higher order river)

Fans in arid to semi-arid regions receive sediment commonly from fluvial processes and sheetfloods (McArthur 1987; DeGraff 1994; Harvey 2011). Fans at higher latitudes and in non-arid regions also receive sediment via fluvial processes, but sheetfloods are not as common in these environments. Debris flows are a more frequent occurrence in these high latitude areas (Rickenmann and Zimmermand 1993 and DeGraff 1994).

### **1.5 Geomorphological Processes on Alluvial Fans**

Net aggradation on many fans is the result of sediment deposition due to a reduction in stream power due to a change in topographic gradient upon reaching the fan. Deposition occurs on these fans when the transporting power falls below the minimum transport threshold (Harvey 2010) Not all fans receive sediment strictly by a reduction of stream power, some fan aggradation is the result of flow expansion from the apex to the toe (Harvey 2010; Blair and McPherson 1994), and other processes such as wind transport and debris flows. As much as alluvial fans are aggradational deposits, their understanding requires a knowledge of the processes that transports sediment to alluvial fans and within their environment. There are two types of sedimentary

processes active on alluvial fans; primary and secondary (Blair and McPherson 1994). These processes are either fluvial processes or a form of mass wasting. In either they construct or enlarge a fan. In contrast, secondary processes modify sediment previously deposited on a fan by the primary processes (Blair and McPherson 2009). Secondary processes are not important to fan construction, and typically result in fan degradation, except in areas recently affected by primary processes (Blair 1987).

### **1.5.1 Primary Processes**

Primary processes that supply the feeder channels of alluvial fans and the fans themselves include rock avalanches or rock falls, debris flows, sheet floods and fluvial processes. Rock avalanches are events with very high energy that consist of large volumes of very coarse angular clasts which break off from rock cliffs due to weathering, undercutting or ground motion (Huggett 2011; Tanarro and Munoz 2012). Unlike other primary processes rock avalanches or rock falls have no water associated with transport (Tanarro and Munoz 2012). Rock avalanches and rock falls transport clasts ranging from centimeters to metres in size, and transport such a large volume that they can potentially build a fan in a single event (Blair and McPherson 2009). Debris flows consist of an unsorted mixture of water and a matrix of coarse clasts. This matrix consists of poorly sorted sedimentary particles ranging from gravel to boulders. Debris flows provide a large volume of material to alluvial fans, and are more frequent than rock falls and rock avalanches, especially in arid and semi-arid regions. These flows are a

response to a rapid input of a large amount of water which causes colluvium to fail (Huggett 2011).

Events that can input large amounts of water into a system would be rapid precipitation from a thunderstorm, heavy rainfall over an extended period of time, or rapid snow or ice melt (Blair McPherson 2009; Harvey, 2010). A sheet flood is a short-duration, catastrophic expanse of unconfined water comprised of gravel and sand (Bull 1972; Blair and McPherson 2009). Sheet floods are instigated by torrential rainfall such as a thunderstorm or from the failure of a natural dam. These floods readily develop on alluvial fans where the flood discharge from the catchment is able to expand. This expansion is promoted by the conical formation of the fans, and begins at the apex or where an incised channel meets the surface (Wells and Harvey 1987; Gomez-Villar and Garcia-Ruiz 2000; Blair and McPherson 2009). Fans in arid regions receive sediment commonly from fluvial processes and sheet floods (Harvey 2011; McArthur 1987; DeGraff, 1994). Fans in higher latitudes and non-arid regions also receive sediment via fluvial processes, but sheet floods are not as common in these environments. Debris flows are a more frequent primary source in high latitude, non-arid regions than are sheet floods (Rickenmann and Zimmermand, 1993 and DeGraff, 1994).

### **1.5.2 Secondary Processes**

Secondary processes typically result in fan degradation and are of little importance to fan construction, although they are the processes responsible for shaping



fans and therefore creating asymmetry. The long periods in between recurring primary processes on alluvial fans makes surficial sediment susceptible to modification by secondary processes (Blair 1987; Blair and McPherson 2009). Secondary processes include wind erosion, neotectonics, particle weathering, pedogenesis and surface and ground water erosion (Blair and McPherson 2009; Harvey 2010). Fine particles on fan surfaces such as clay, silt and sand are susceptible to wind erosion and entrainment. Effects of wind can mould protruding clasts into ventrifacts by abrasion, or transport sand and silt to or from a fan surface (Al-Farraj and Harvey 2000). Neotectonics are common where there are fans developed along a seismically active mountain front. Tectonic uplift can affect the context and settings of alluvial fans by changing gradient and/or base level characteristics. Base level and gradient change can cause aggradation on a fan by increasing the slope of a catchment or the fan itself (Silva *et. al.*, 1992; Harvey 2000). Steeper catchments would result in more sediment being eroded and supplied to a fan, whereas a steeper fan would cause aggradation on the distal end (Silva *et. al.*, 1992; Harvey 2000). In contrast, tectonic subsidence can lower the gradient of fans and cause the fan to become larger in area (Viseras *et. al.*, 2003).

Many types of physical and chemical weathering modify fan sediment including salt crystal growth in voids, exfoliation, oxidation, hydrolysis and dissolution (Goudie 2004). These reactions take place on the surface of fans and break the larger clasts down making them prone to aeolian effects, thus degrading the fan (Goudie 2004; Blair and McPherson 2009). Bioturbation can potentially homogenize the deposits on a fan or plant presence can break down the stratigraphy of a fan with their root systems. Shallow groundwater flow may create the conditions required for plant growth, and since alluvial

fans serve as important groundwater conduits (Huston 2002) bioturbation is especially common on fan regions that support flora with deep root systems such as glaciated valleys (Huston 2002).

As suggested by Blair and McPherson (2009) perhaps one of the greatest misconceptions associated with alluvial fans is the thought that fans are constructed by the presence of braided streams on the face. These braided streams are secondary processes; they winnow and remould the deposits left behind by primary processes and occur chronologically in between said primary processes. These braided streams look like that would be supplying the fan with sediment, but they are not large enough to transport the amount of sediment required to surpass the amount of sediment they remove from the fan (Blair and McPherson 2009).

## **1.6 Alluvial Fan Asymmetry in Literature**

Alluvial fans in arid to semi-arid regions have been the dominant topic of recent published fan literature. Until about 40 years ago most research literature regarding alluvial fans came from the American Southwest (Blair and McPherson 2009; Harvey 2011). Alluvial fans are present in many global environments, but fans in arid and semi-arid environments have been studied the most due to their excellent exposure and ease of access (Blair and McPherson 2009). Since the 1960's fans in the semi-arid regions of western North America and, southern Europe have been the main focus of alluvial fan research (Blair and McPherson 2009). Furthermore, it has only been since the late

1970's that alluvial fan research has expanded to the higher latitudes of North America (Ritter and Ten Brink 1986).

Higher latitude alluvial fans are more susceptible to toe cutting or axial river modification because the valleys where fans typically form have rivers or streams, unlike the arid regions of the American Southwest where there are no rivers (Leeder and Mack 2001). Observations in this study have shown that the presence of an axial river seems to have a correlation with planform asymmetry. Since the presence of axial rivers modifying alluvial fans is very uncommon in arid to semi-arid regions, the topic of fan asymmetry has not received a lot of attention.

In scientific publications the idea of fan asymmetry of any kind has been hard to find. A direct reference to fan asymmetry in any published research for this study has not been found at all. Though not directly described as fan asymmetry, there are a few research papers that do indirectly mention processes that could cause fan asymmetry, and some even acknowledge the possibility of one half of a fan being unequal in area to the other. So far the most direct published reference to fan asymmetry is made by Hashimoto (2008). While using GIS to analyze depositional slope change at alluvial fan toes, Hashimoto mentioned that measuring gradient along a single line upon a fan face may yield various results "...because an alluvial fan is not always symmetric..." (Hashimoto 2008, pp. 124). Hashimoto did not expand further on the idea of a fan asymmetry, but his article does have some interesting similarities to this study. These similarities include measuring the longitudinal slope change on alluvial fans and also measuring the slopes of the lowland areas on which the fans developed.

Aside from Hashimoto's article, mentions of symmetrical fans in planform or even planform symmetry have been indirect at best. Leeder and Mack (2001) described lateral erosion ('toe-cutting') of alluvial fans by axial rivers in great depth, a process that seems to be present at the toe of all the asymmetrical fans in this study. Leeder and Mack (2001) further describe how sediment is eroded from the upstream side and carried downstream by the axial river present, but do not mention anything about the consequent shape of fans in the presence of lateral erosion. Lateral erosion has also been acknowledged by Blair and McPherson (2009) and Harvey (2011) as a secondary process that degrades an alluvial fan. This secondary process is illustrated by Harvey (2011), but again there is no mention of alluvial fan asymmetry.

## **1.7 Study Questions and Goals**

The goals of this research are to provide some insight into the idea of fan asymmetry and to try to make a connection between fan asymmetry, fan gradient and surface stream flow distribution. Furthermore, if there is a statistically significant degree of asymmetry in alluvial fan planform morphology, this study seeks to provide a valid explanation as to why it would occur. In this study the primary research question is: Is there a statistically significant degree of asymmetry on alluvial fans in planform? In addition, there are two secondary research questions: 1) Is there a significant statistical difference in gradient when comparing the length profiles of the upstream and downstream sides of the chosen fans and 2) Is there a non-random distribution of surface streams on the fan surfaces? More specifically this study seeks to determine

whether fans within Kluane National Park, Yukon, and the Wrangell and Kenai Mountains, Alaska, have longer downstream lengths than upstream lengths in relation to axial rivers at their toe.

### **1.8 Preview of Thesis**

The next chapter will give some background information pertaining to the study areas used for this research project. Chapter 3 will give a brief description of the valleys that contain groups' fan that have been selected for study. Geological characteristics of the study areas will be discussed, along with a brief history of glaciation and a brief history of climate. The third chapter will focus on the methods used to select fans, create the data collection layout, gather data, produce morphological indices and perform statistical tests. Chapter 4 will address the primary research hypothesis concerning difference in lengths between fan sides in planform. Chapter 5 will address the secondary research hypotheses, regarding the difference in gradient and surface stream distribution. There will be a discussion in Chapter 6 and a new alluvial fan model will be presented, and a conclusion will be made.

## CHAPTER 2

### STUDY AREAS

Groups of alluvial fans were studied within the valleys of Yukon, Canada, more specifically Kluane National Park, Wrangell – St. Elias National Park and Kenai mountains of Alaska, USA (Figure 1). All the fans used in this study had no interaction with neighbouring fans, and the available imagery of the valley that contained the fans selected for study was of high enough quality to identify an alluvial fan from other topographic features. These criteria were important in the process of fan selection ensuring a high level of accuracy and ruling out the possibility of a fan being asymmetrical because of the constraint of an adjacent fan; this is explained further in section 2.1.

#### **2.1 General Study Area Geology**

The valleys of Kluane National Park and Alaska are located within the Insular Belt which consists of the Wrangellia, Alexander, and the Yakutat terranes (Plummer 2007). These terranes are the last to dock against western North America and they are the farthest western extent of the Cordilleran mountain belt. The collision of these terranes against the North American craton has created high compressional forces that have thrust crustal rock upwards. This compression has resulted in a highly mountainous

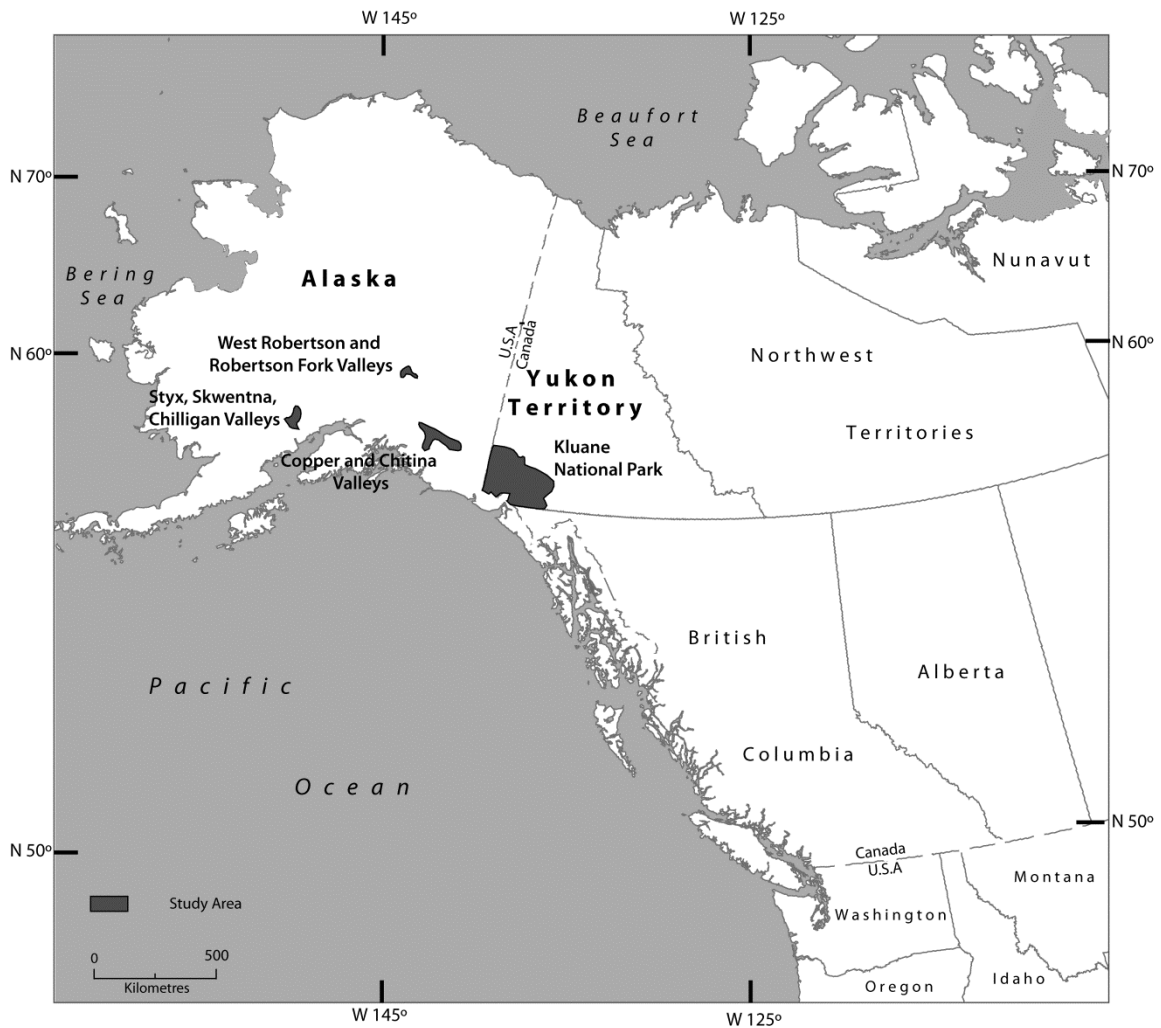


**Figure 2.** *Study Area, Alaska and Yukon*

region from the Pacific Ocean eastward to the boarder of the Yukon in the North, and Alberta in the South. The Insular Belt is made up of late Paleozoic sedimentary and intrusive rock that has been subject to erosion in North America since its docking around 300 million years ago (Pennsylvanian Sub period).

## 2.2 Yukon Group

The Yukon group consist of 38 fans. For convenience of referencing, sub-groups of fans were created by grouping fans that are within the same valley. The sub-group is then named after the respective valley (for example, fans in Slims Valley are called the Slims sub-group). There are six major valleys within Kluane National Park with fans selected for this study: Alsek, Disappointment, Donjek, Kaskawulsh and Slims. These valleys are mapped and shown in Figures 3, 4, 5 and 6, Figure 4 in particular gives a detailed scaled representation of fans from the northwest section of Kaskawulsh valley. All of these valleys are glaciated, with their respective glaciers of the same name present at the valley head. Major glaciers in the area such as Kaskawulsh glacier feed the rivers that flow along the toe of the fans in each valley. The source basins for all the fans in the Yukon are tributaries of the major valleys mentioned above. All the tributaries and major valleys are located in the St. Elias Mountains within Kluane National Park. The St. Elias Mountains are a coastal mountain range located along the northern margin of the Cordilleran ice sheet (Jackson and Clauge 1991) in the south western corner of the Yukon Territory and are mainly comprised of intrusive granodiorite and quartz diorite. The St. Elias Mountains like the rest of the Yukon, have been repeatedly affected by the northern Cordilleran ice sheet before its furthest extent in the Late Wisconsin (Ward *et. al.* 2007). Although termed an ice sheet, Ward *et. al.* (2007) explained the Cordilleran ice sheet is better described as an ice complex, composed of a series of coalescing valley glaciers and piedmont lobes whose ice flow was strongly controlled by topography. The retreat of this ice sheet 10 000 years B.C.E. provided much of the sediment for alluvial fan development in the Yukon and Alaska.



Being situated at a high latitude the Yukon group is subject to a continental polar air mass with winds typically coming from the east. The climate in the region is semi-arid due to the orographic effect of the St. Elias Mountains situated to the southwest of the study area, creating a rain shadow. In addition, sites to the northwest situated in the Central Yukon Basin where elevations are lower than the St. Elias Mountains, winter temperatures are colder, black spruce is more abundant, permafrost is more continuous, and the effects of the Aleutian Low over the Gulf of Alaska are less pronounced (Wahl et al., 1987).

The closest weather station is at Burwash airport. The station is at 806m and is located just north of the Yukon group also inside Kluane National Park. The mean annual precipitation at Burwash is 279mm, most of which (68%) falls during the summer months as rain (1971-2000 climate normal; Environment Canada, 2009). Snowmelt and rainfall is the highest in late spring to mid-summer, which creates high amounts of runoff during the months of June and July. Mean annual temperature at Burwash is -4 °C with the coldest month being January (-22 °C on average) and the warmest month being July (12 °C on average) (1971-2000 climate normal; Environment Canada, 2009).

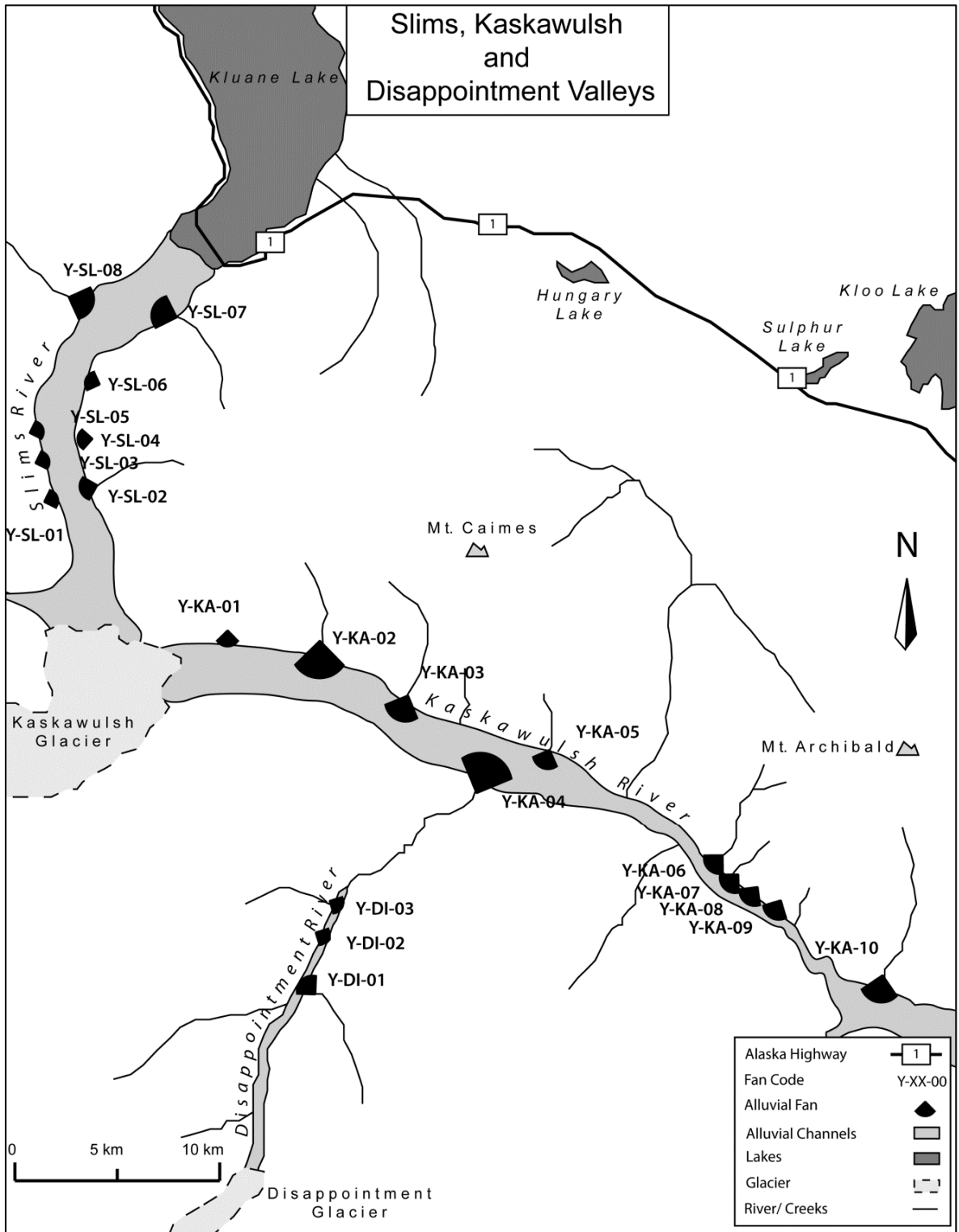
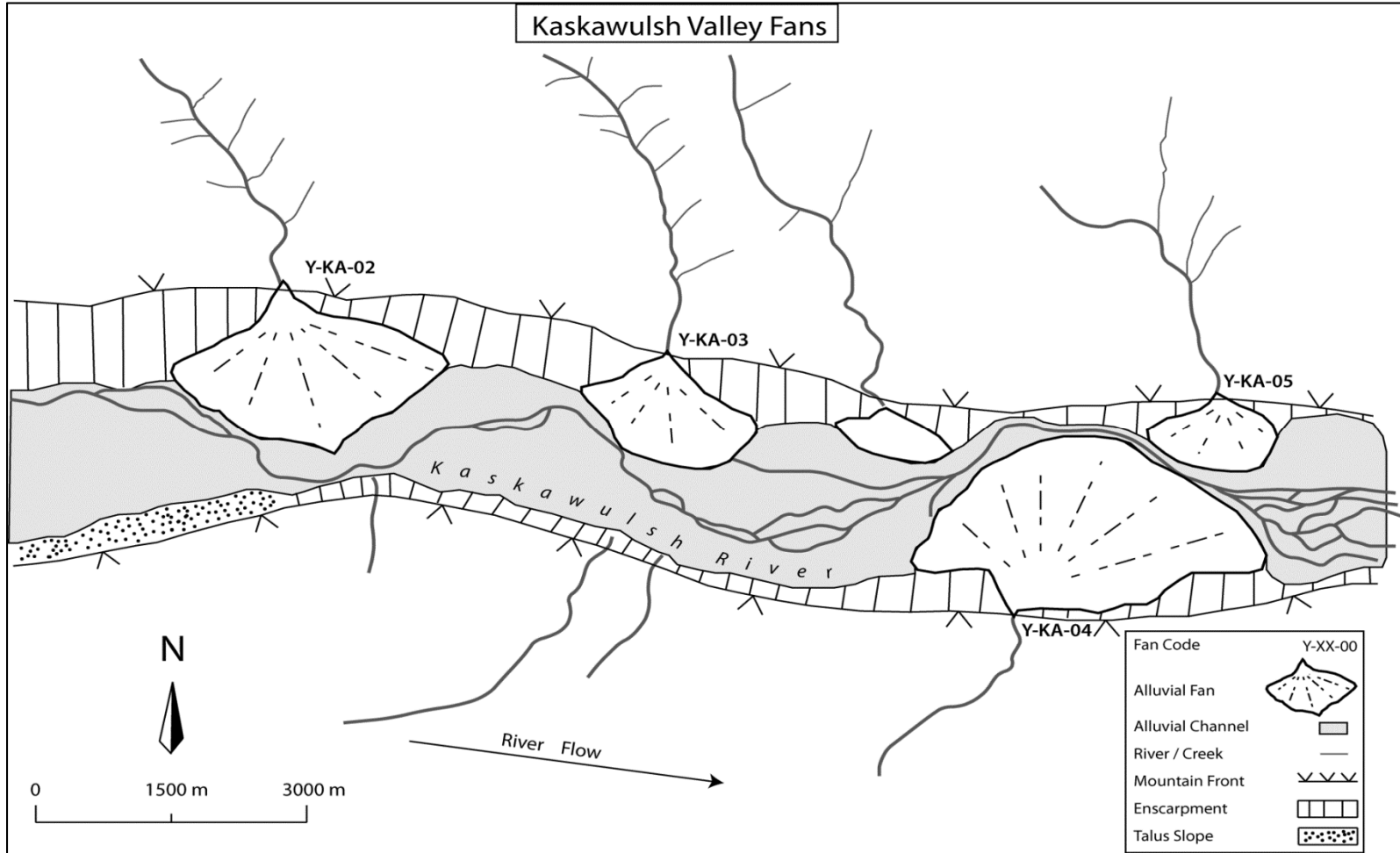


Figure 3. Slims and Kaskawulsh valleys and subsequent fan subgroups.



**Figure 4.** *Small scale planform view of the western section of Kaskawulsh valley*

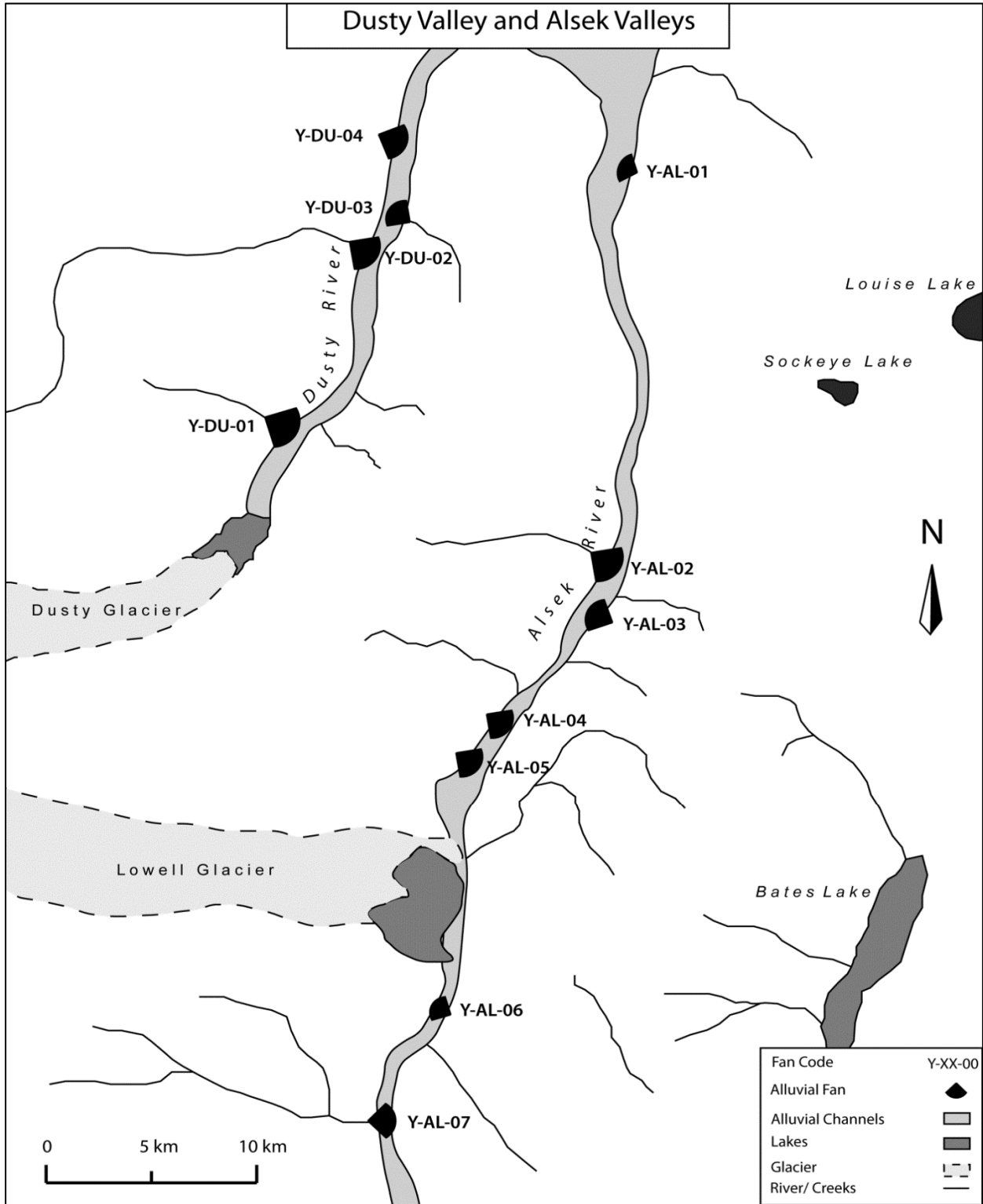


Figure 5. Dusty and Alsek valleys and subsequent fan subgroups.

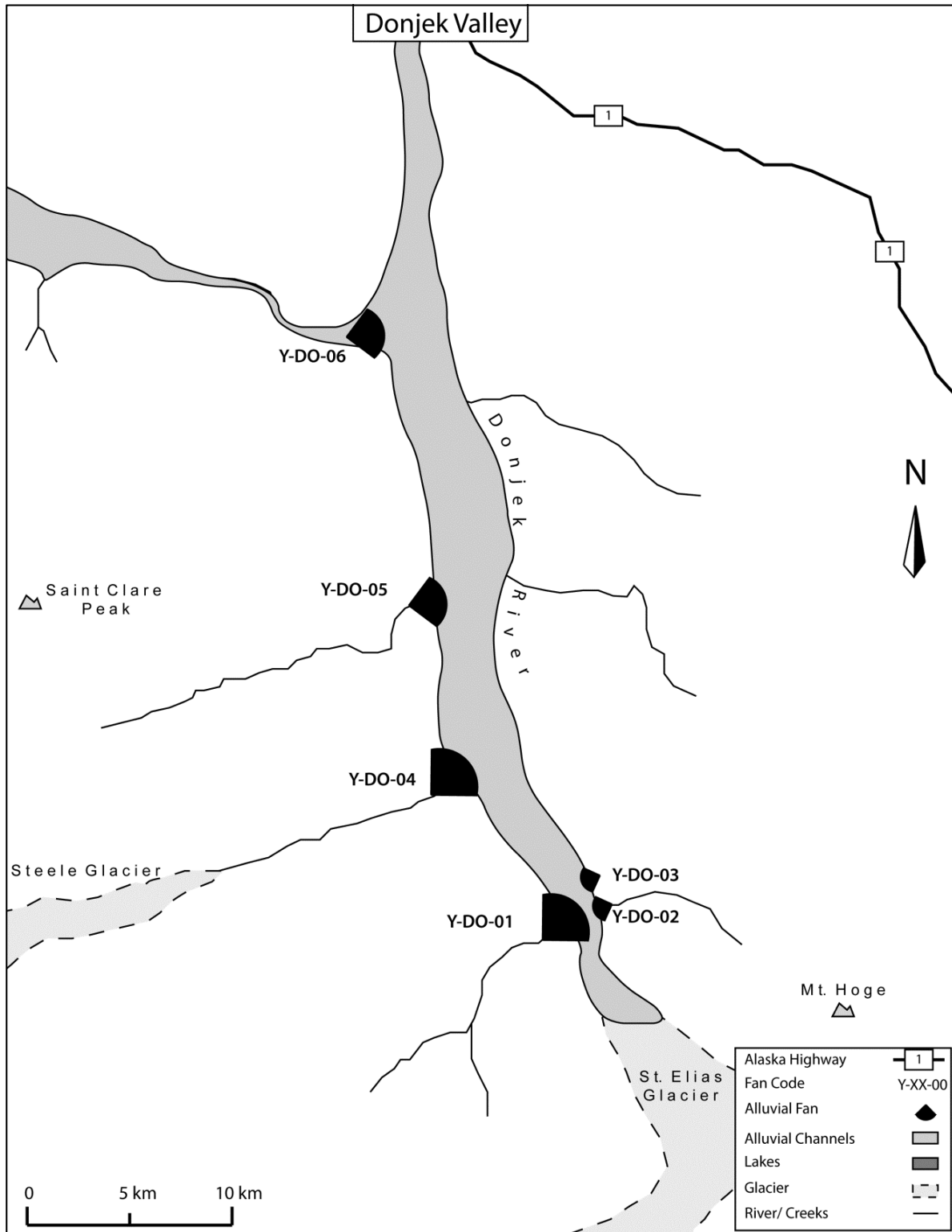
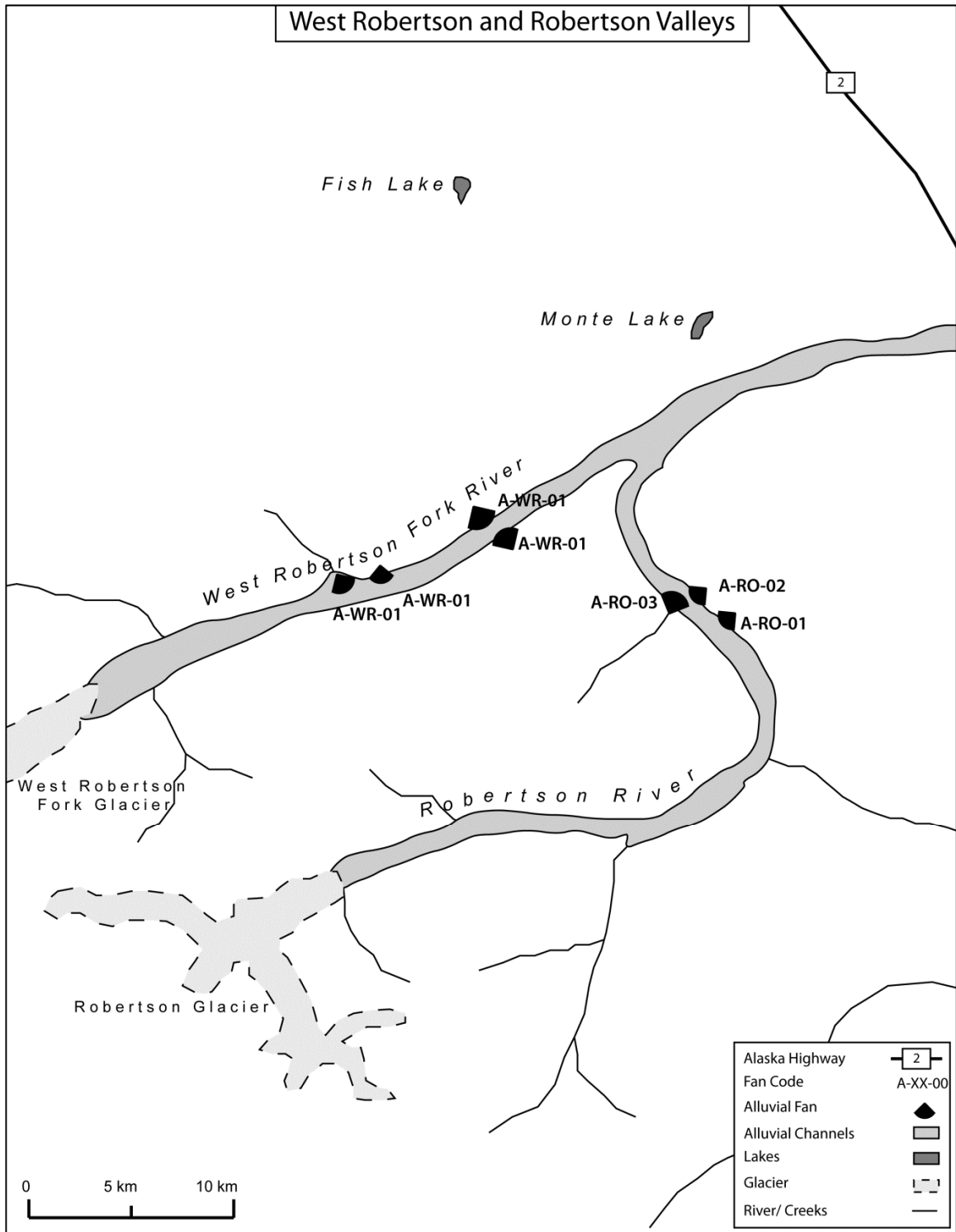


Figure 6. Donjek Valley and subsequent fan subgroup

### 2.3 Alaska

The Alaska group consists of 32 fans and like the Yukon group the fans are broken down into smaller sub-groups named after the valleys they occupy. The Alaska group are broken down into seven sub-groups which are in the: Chilligan, Chitina, Copper, Styx, Skwentna, Robertson and West Robertson Fork valleys, all mapped in Figure 7, 8, 9, and 10. These valleys are located in the Wrangell – St. Elias National Park / Mountains in the western corner of Alaska and the Kenai mountains directly west of Anchorage. Similar to the Yukon group, most valleys with selected fans have glaciers at their head feeding the axial rivers. The history of glaciation in Alaska is also very similar to that of the glaciation history in the Yukon. As explained above, the Wrangell Mountains and Kenai mountains are located along the northern extent of the Cordilleran ice sheet that advanced and retreated with coalescing lobes and piedmonts until its last extent 10,000 years B.C.E. (Jackson and Clauge, 1991). With the high amount of precipitation and low temperatures coming from the maritime polar air mass in the Bering Sea, these coastal mountain ranges of Alaska are ideal locations for glaciers to reside. Even though there is high precipitation along the coast of Alaska, the fans selected for this study are located on the leeward side of the coastal mountains in a rain shadow. The rain shadow drops the mean annual precipitation of the group of fans in the Kenai Mountains to 464mm from 1700mm, with most of that falling from August to October. The same effect is present in the Wrangell mountains (where the mean annual temperature is 2°C) (1981-2010 Weather Data; NOAA, 2010).



**Figure 7.** West Robertson and Roberson valleys and subsequent fan subgroups in the Wrangell Mountains

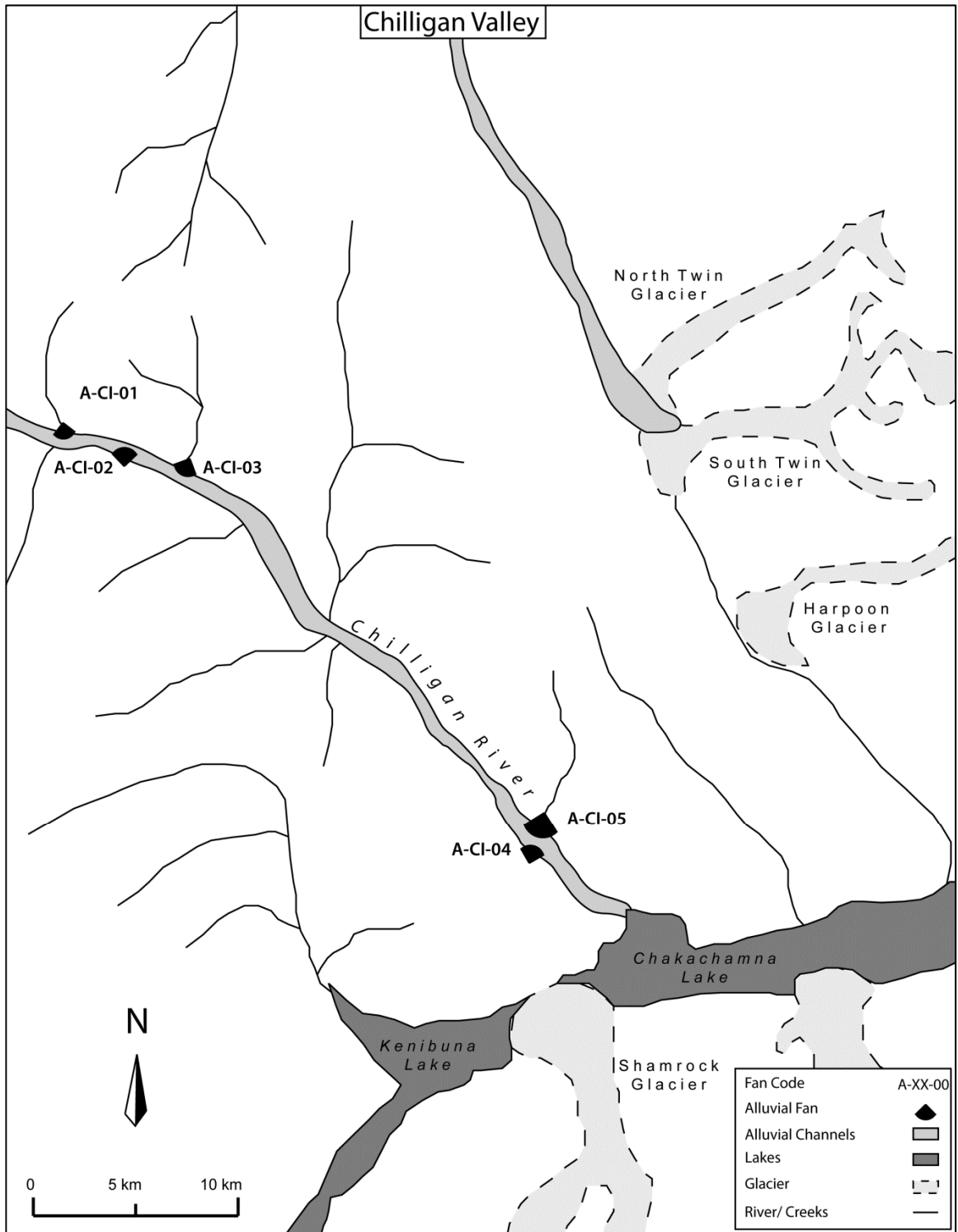


**Figure 8.** *Chilligan valley and subsequent fan subgroup in the Kenai Mountains west of Anchorage*



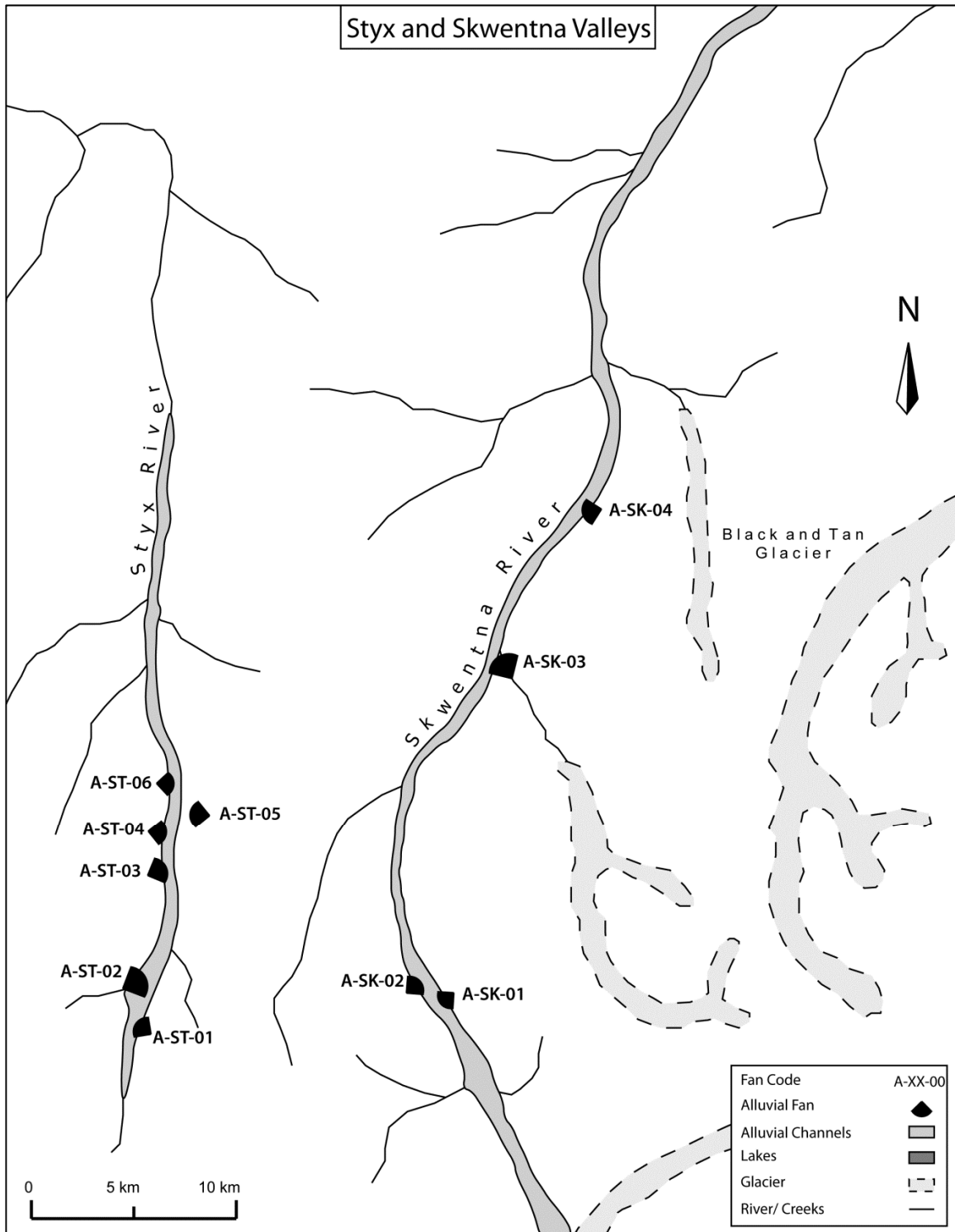


**Figure 9.** *Styx and Skwentna valleys and subsequent fan subgroups, in the Kenai Mountains west of Anchorage*

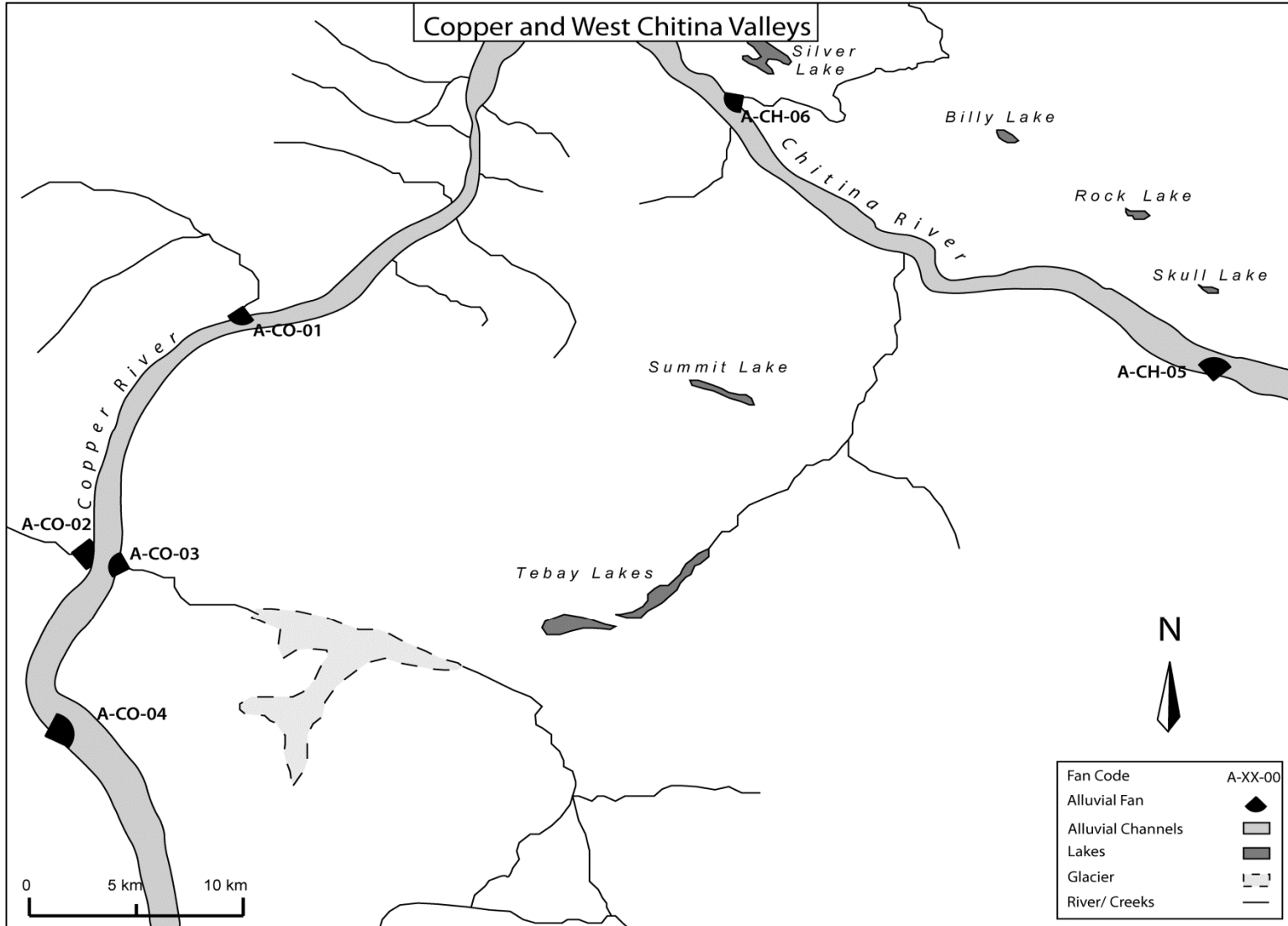


**Figure 10.** Copper and Chitina valleys and subsequent fan subgroups in the Wrangell Mountains west of Klwane

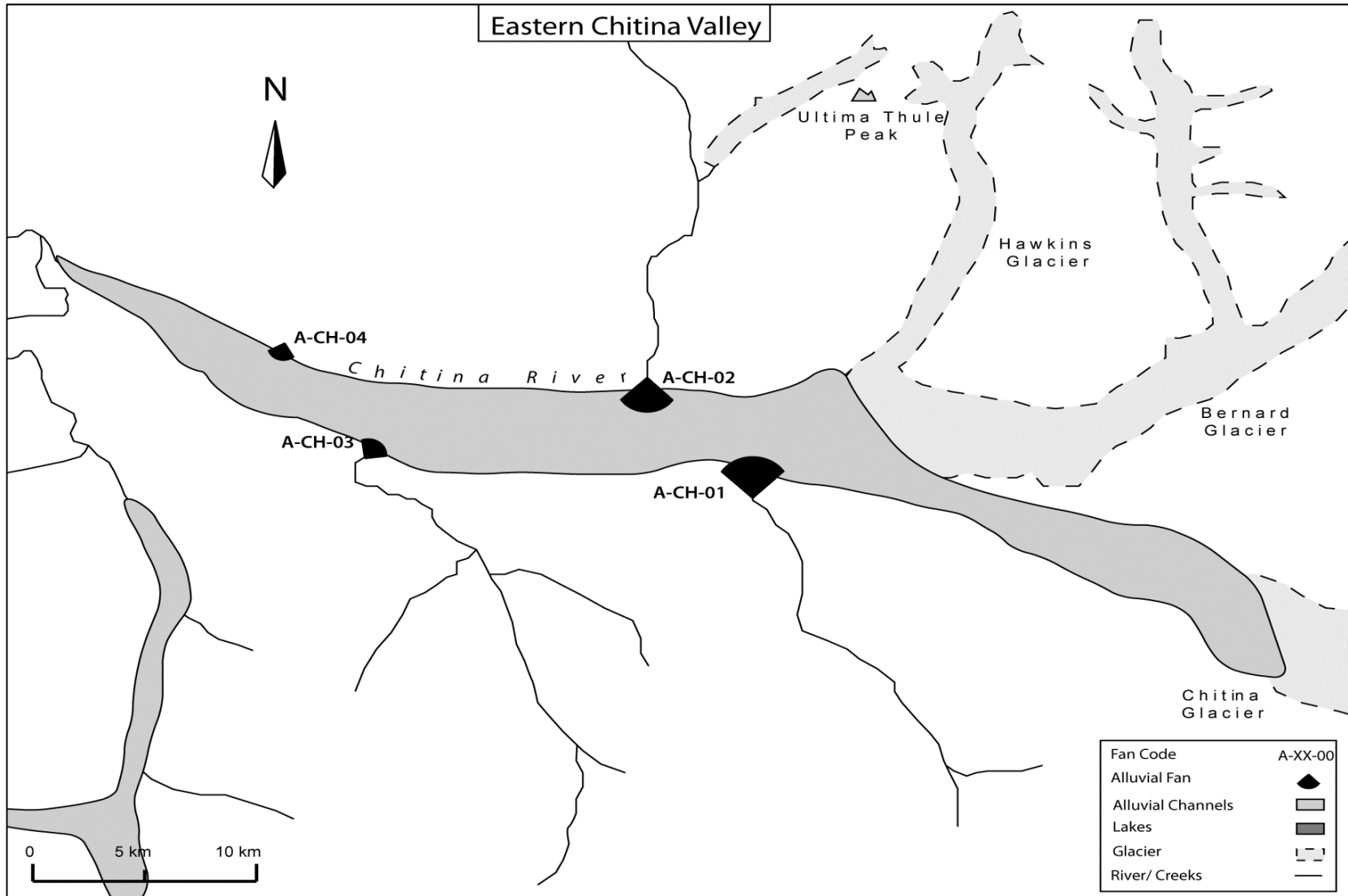


Figure 11. East Chitina valley and subsequent fan subgroup

The mean annual temperature in both regions is 2 °C with the coldest month being January (-9 °C) and the warmest month being July (13 °C). Vegetation in both regions is prominently boreal forest that includes white spruce, paper birch, aspen and balsam poplar. On poorly drained landscapes or at the tree line (600-700m), white spruce is replaced by black spruce (Muhs 2004).

The coastal mountain ranges of Alaska are still being uplifted from the collision and subduction of the Pacific Plate and the North American plate, and have an elevation range of about 1600m (700m-2300m) (Nicholas, 1958). These mountains are mostly comprised of sedimentary and volcanic rocks that include: gray argillite, greywacke, quartzite and quartzite schists (Nicholas, 1958). In general the rock in this region is Precambrian in age but contains sediment that has been deposited in the Holocene after the retreat to the Cordilleran ice sheet.

## CHAPTER 3

### METHODS

#### 3.1 Alluvial Fan Selection

Not all fans within Kluane National Park, St Elias National Park and the Kenai mountains were used in this study. For a fan to be incorporated into the sample it had to meet a set of criteria. Each criterion that was set to ensure that each fan was distinguishable from the mountain front and other depositional features (like a talus slope) and had adequate accommodation space, and unrestrained development. The criteria that had to be met were: a) there is an absence coupling (two or more fans were not joined together); b) the valley in which any fan has formed is wide enough that the toe of the fan was not touching the opposite valley wall; c) there is only a single feeder channel developing a single fan; and finally, d) the fan was distinguishable from the mountain front with the imagery available.

Fans that were coupled or had their toe development restricted by another fan were not included. These fans were not included because toe sharing and coupling can create an asymmetrical formation as a result of restricted development and not due to secondary processes. This study focused on processes that changed a symmetrical fan into an asymmetrical shape. Furthermore, only one single feeder channel was important in the selection of the fans. The presence of more than one feeder channel feeding a single fan can create a bajada (a continuous slope of sediment, or multiple fans overlapping laterally) with no clear apex, similarly two feeder channels too close together or overlapping can create coupling.

The last and possibly most important factor that had to be met was regarding the image quality provided through Google Earth. Since Google Earth is a mosaic of satellite images, there is a range of image quality, and in some cases a range of quality on a single fan. To ensure the highest accuracy, imagery for a single fan had to have a high enough resolution and detail to distinguish between the fan surface, the mountain front and other topographic features. The selection processes (using the criteria mentioned), resulted in the identification of 70 suitable fans for this study.

### **3.2 Data Collection Layout**

After suitable fans were selected a data collection layout was created as a guide for measurements along the fan surface. The data collection layout was the guide from which all of the data collected and used in this study came. The first step in the creation of the data collection layout was to get a suitable image from Google Earth with an appropriate scale for the size of the fan. A single scale was not used for all fans because of their varying size; larger fans had smaller scales and smaller fans had larger scales to increase precision while performing measurements. The images of the fans were imported into Adobe Illustrator from Google Earth with their corresponding scales, and outlines were drawn around their boundaries. Figure 12 shows what the outline created in Adobe Illustrator looks like when seen in Google Earth. The second step shown in Figure 13 was to draw two edge lines extending from the apex to the corners of the fan so it was possible to measure the angle of the fan arc. The corner of the fan was determined as the spot along the outline where the fan toe meets the

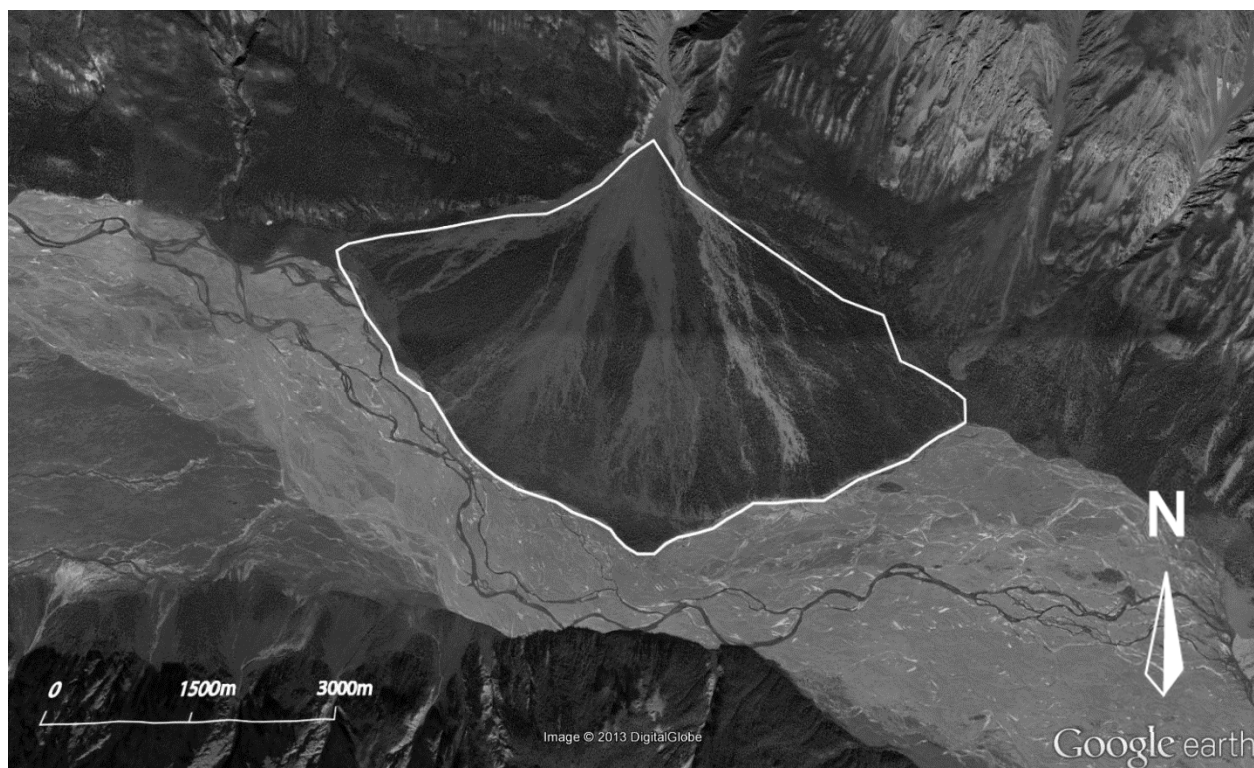


**Figure 12.** *Outlined Alluvial fan (Kaskawulsh Valley; Y-KA-02) from Adobe Illustrator imported back into Google Earth (Google Earth, 2013).*

mountain front. After the edge lines are drawn the fan arc angle between them is measured.

The fan arc angle is the degree of the angle between the two edge lines.

Step three was dividing the recorded fan arc angle into five geometrically equal sectors. Lines were drawn (Figure 14) from the apex beyond the toe at equal intervals. The intervals at which the lines were placed came from the product of the fan arc divided by five. An uneven number of sectors was used so that there was one sector that would contain the geometric centre of the fan (in this case sector three is the middle shown in Figure 14), and also the middle of sector three would be the geometric centre of the fan and not the boundary line between two sectors. Furthermore, if there was a surface stream flowing down the centre of a

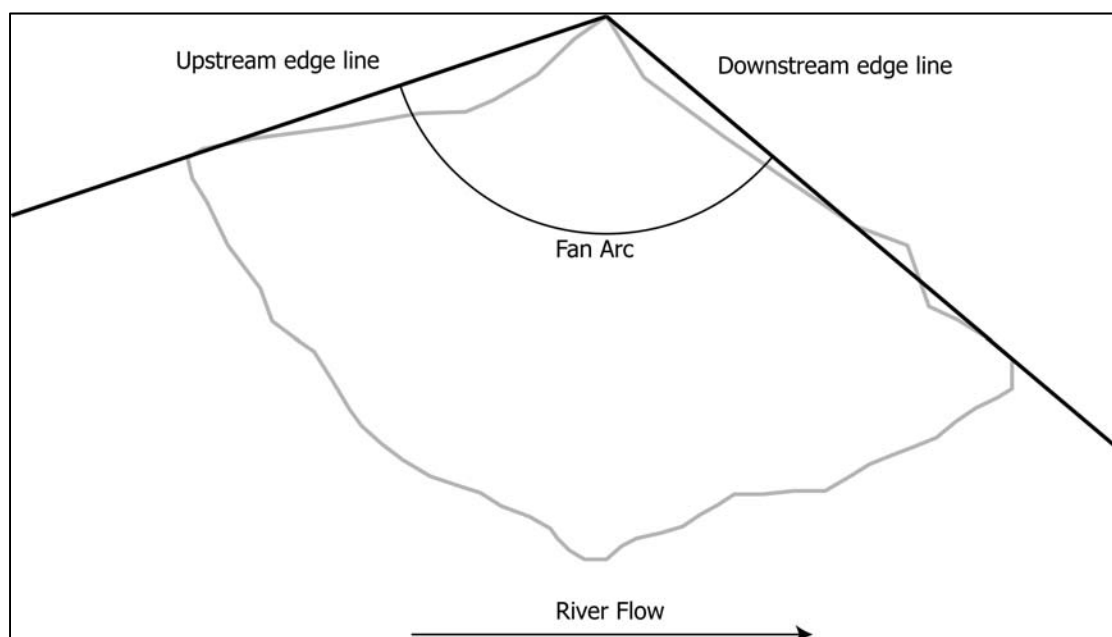


**Figure 13.** *Outlined Fan (Y-KA-02) in Adobe Illustrator. Upstream and Downstream edge lines are drawn from apex to fan corners; these lines make it possible to measure fan arc.*

fan it could be said that it occupies one sector. Upon initial observation it seems there is a high frequency of fans with streams that flow down their geometric centre; thus, an odd number of sectors would cut down on the discrepancies between sectors when a stream flowing down the geometric centre (see Figure 14). There will still be streams that straddle the dividing line between two sectors, and a stream may meander between two sectors, so the sector that has the most of the stream in it will be considered the sector which the stream flows through. Now that an odd number of sectors has been decided upon to divide up the fans, how many sectors should be used? Five sectors were chosen to divide up the fans because five sectors provide adequately sized outer sectors so that the geometric middle of the outer sectors could serve as a buffer from the extremely variable edge boundary of the fan.



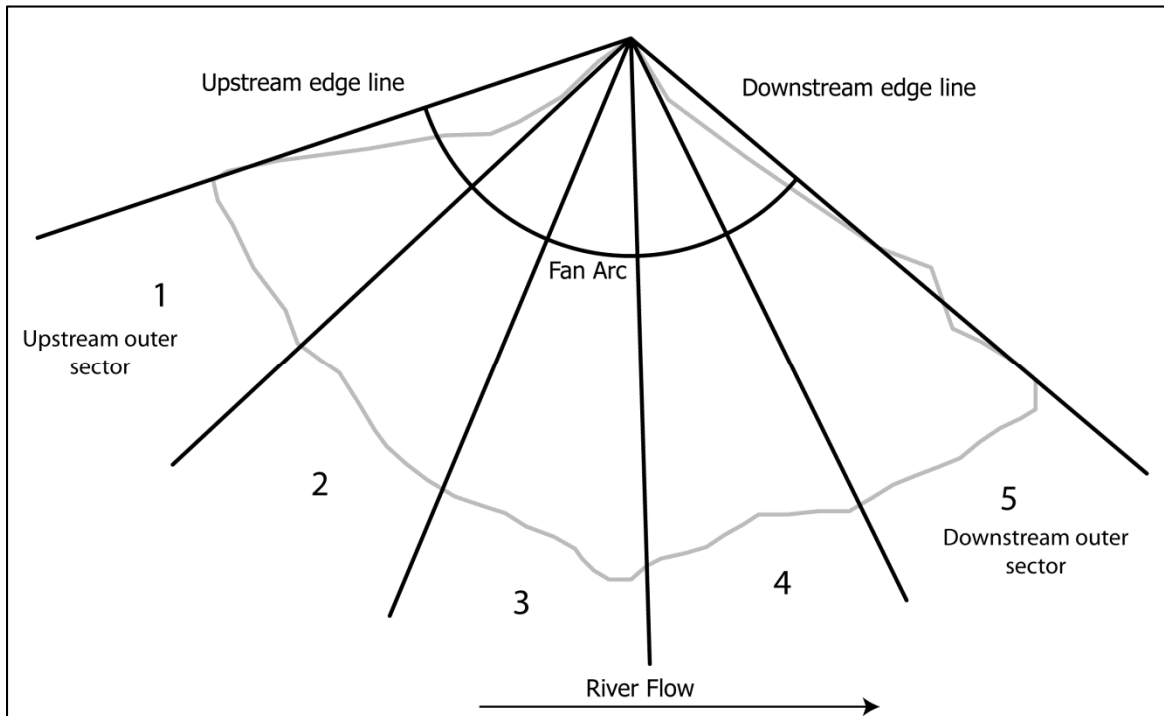


**Figure 14.** Five equally divided sectors are added at equal intervals. Intervals are found by dividing the fan arc angle by 5.

Illustrated in Figure 15 is the fourth step of the data layout creation. In this step lines are drawn from the apex to the toe, through the middle of the two outer sectors. The outer sectors are referred to the upstream edge and downstream edge depending on which side of the fan the outer sectors are on with reference to direction of stream flow at the base of the fan. The lengths of the lines that run through the centre of the upstream and downstream sectors are equal, and are dependent on the

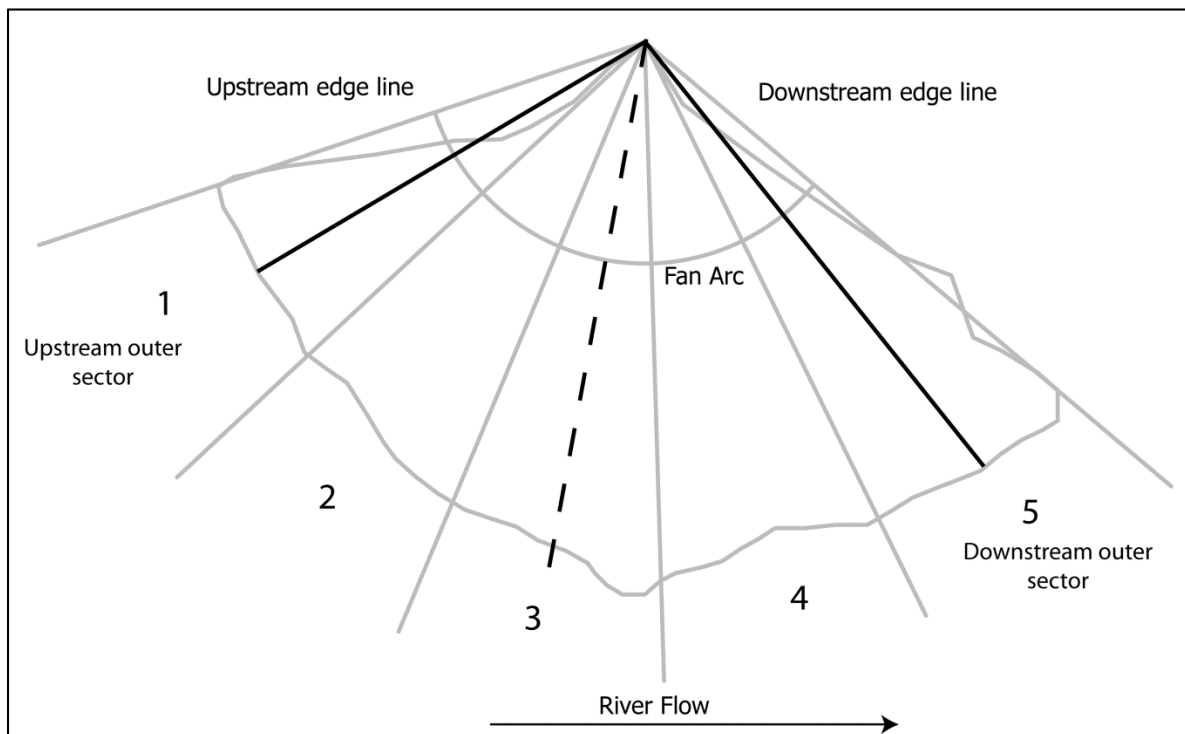


**Figure 15.** Length profile guide lines are added in sectors 1 (Upstream) and 5 (Downstream). Also added, a centre line (sector 3) and the mountain front lines.

upstream length. The line drawn from the apex through the middle of the upstream sector is copied and rotated and placed in the middle of the downstream sector also using the apex as the starting point. These length lines used to measure asymmetry are placed through the middle of the outer sectors to get a more precise average of a side length. Hashimoto (2008) uses a similar technique in which he calls the area between where the measurements have been taken and the edge of the fan, buffer zones. They are employed so that the measurements and corresponding data will provide a more precise average representation of the fan.

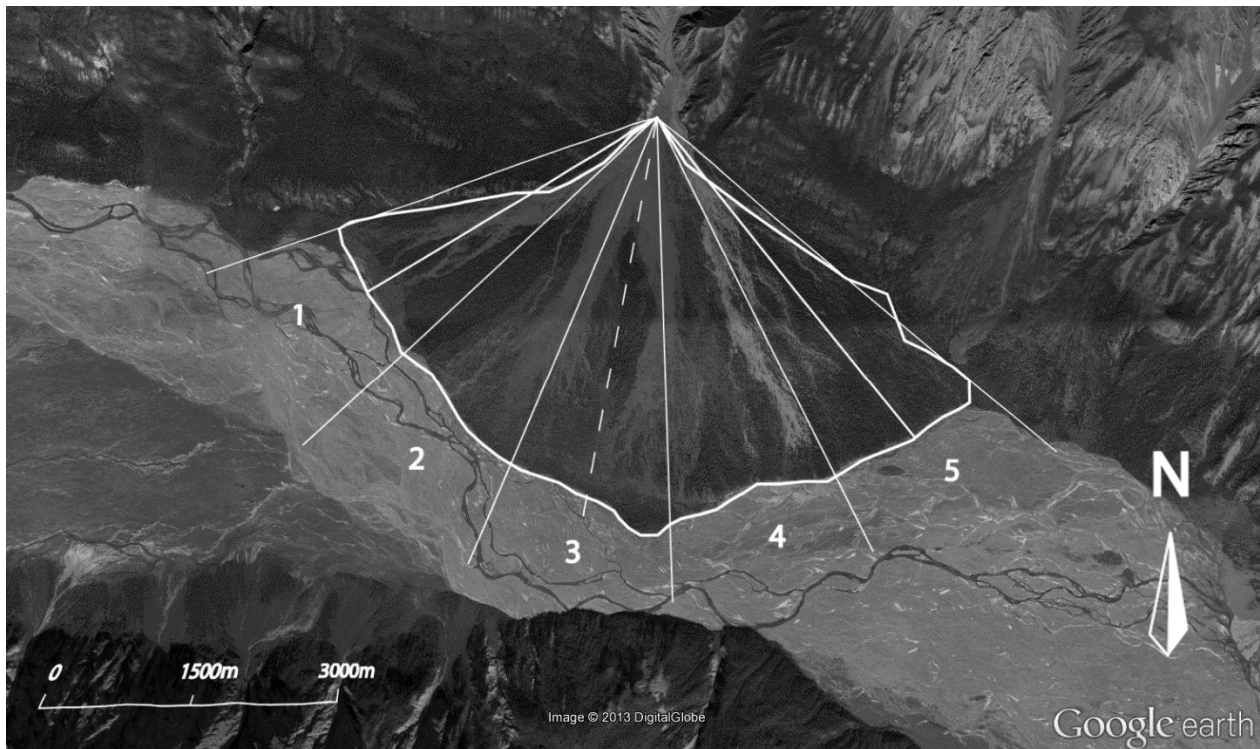


**Figure 16.** *Completed data layout imported into Google Earth from Adobe Illustrator (Google Earth, 2013).*

The fifth step also shown in Figure 15, is to draw lines used for the valley width and valley gradient data collection. A dashed line is drawn through the geometric centre of the fan which happens to be the middle of sector three. This line extends beyond the fan toe, and will geometrically split the fan in half.

The sixth and final step is to import the finished data collection layout back into Google Earth shown in Figure 16. Since the outline has been traced in Google Earth and the outline has not been altered in anyway, when it is imported back into Google Earth there is no need to stretch the image to make it fit over the fan it is made for, therefore preserving accuracy.

### 3.2.1 Data Collection and Measurements

After the data collection layout is imported back into Google Earth and placed over a given fan, measurements are taken and recorded. The data collection layout provided a guide to gather data for an asymmetry index calculation which required the measurement of the upstream and downstream lengths, with the results to be shown in a histogram. The data collection layout also provided data for a gradient calculation and a surface stream distribution histogram.

To collect data for asymmetry index calculations, the lengths profiles of each side were measured in Google Earth with the 'Ruler' application; measurements were made from apex to toe along the line drawn through the geometric centre of the outer sectors one and five in. Fan gradient calculation uses the elevation measurements taken at the end of the same lines in sectors 1 and 5 used to find side length. A gradient calculation is also done for the valley which the fan occupied. Like fan gradient, elevation and distance measurements were required for a valley gradient calculation. Valley distance measurements were taken from 1:50 000 topographic maps received from Natural Resources Canada and USGS. Distances were measured from a point on the line drawn along the geometric centre of the fan that extends beyond the toe to the nearest upstream and downstream contour following the river valley. At the nearest contour upstream and downstream from the fan, both distance and elevation were measured in metres.

## CHAPTER 4

### ALLUVIAL FAN ASYMMETRY RESULTS AND DISCUSSION

As mentioned earlier in this study, alluvial fan asymmetry is not a subject that has received much attention in the past, so the goal of this research question is not only to determine whether a statistically significant degree of asymmetry exists within the dataset but also to provide a working method that could be applied to any alluvial fan in any region around the world. The question is; do the alluvial fans in Yukon (Kluane National Park) and Alaska (Wrangell Mountains and Kenai Mountains) as a group display a statistically significant degree of asymmetry?

#### 4.1 Calculating Fan Asymmetry and Hypothesis Testing

When examining fans in planform, fan asymmetry in this study is the difference in distance from apex to toe between the upstream and downstream sides. Section 3.2.1 describes how the lengths of each side were found. With the lengths of the upstream and downstream sides known, it was possible to compare each side to find a difference in length profiles. To express fan asymmetry, a simple calculation was performed to receive an asymmetry index (AI). The AI is the result of the division of upstream length ( $L_U$ ) and the downstream length ( $L_D$ ) of the fan surface, which is shown in Equation 1:

$$AI = L_U/L_D$$

**Equation 1. Asymmetry Index Calculation**

With AI values found for all 70 fans it was possible to make a simple histogram to represent the distribution of fan asymmetry. The resulting histogram (Figure 17) has a neutral value of 1 meaning any asymmetry index with a value of 1.0, is considered to be symmetrical or very close to symmetrical. A fan that has an asymmetry value that is less than 1 has a longer surface length upstream than downstream, and vice versa with fans with values larger than 1. With that in mind, the mean AI value of the resulting histogram (Figure 17) is 1.23, which also shows a higher frequency of distribution of fans that have an AI greater than 1.0, than fans that have an AI less than 1. This histogram shows that fans in study areas of Kluane National park, and Alaska have a higher frequency of fans with a longer downstream profile than upstream profile.

To determine if the mean AI value is significantly greater than 1.0, thus signifying asymmetry, the AI values were tested under a normal curve employing a one-tailed hypothesis test with a significance level of 0.05. A one tailed hypothesis was used to test the observation that fans in Kluane National Park , Wrangell Mountains and Kenai Mountains have longer length profiles downstream than upstream. The null hypothesis is:  $AI = 1$  and the alternative is:  $AI > 1$ . Equation 2 shows the calculation used to find the Z-score to test the alternative hypothesis (Burt, *et al.* 2009).

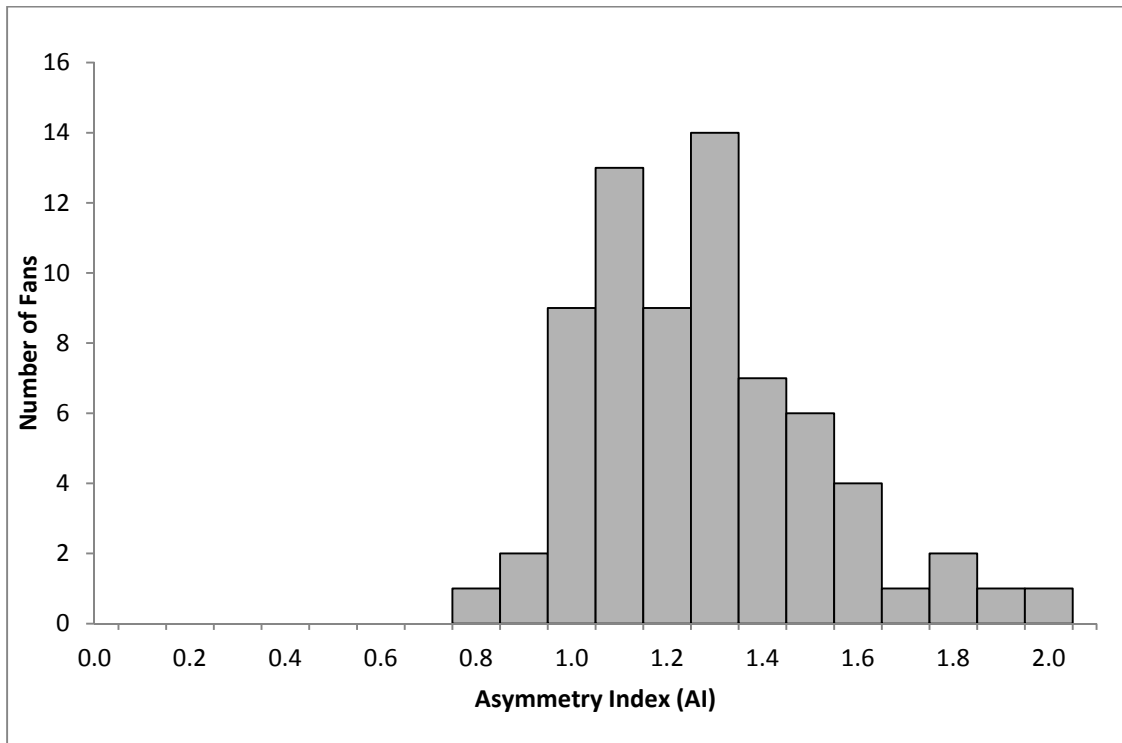


**Figure 17.** *Histogram of Asymmetry Index distribution*

$$Z - Score = \frac{\bar{x} - H_o}{\sigma/\sqrt{n}}$$

**Equation 2.** Z-score equation for one-tailed hypothesis test (Burt, Barber and Rigby 2009).

The average ( $\bar{x}$ ) and the standard deviation ( $\sigma$ ) of all the AI's are found and used in the z-score equation.

## 4.2 Asymmetry Results and Discussion

A one-tailed hypothesis was employed to test specifically if the downstream side of the fans were longer than the upstream side. The reason for only using a one-tailed hypothesis test was because when observing the results presented in Figure 17 there is a high frequency of AI values above 0. Therefore employing a one-tailed hypothesis test to confirm if indeed the downstream length profile is significantly longer than the upstream side makes sense. The breakdown of the one tailed hypothesis test is shown in Table 1 and Figure 18 shows the results under a normal curve. As shown in Figure 18, the z-score provided by the hypothesis test (7.93) falls well beyond the critical z-score value (1.64). With a z-score of 7.93, the null hypothesis (there is no significant difference in length profiles in Alaska and Yukon fans) is rejected in favour of the alternative hypothesis (the length profile of fans in this study is longer downstream than upstream).



|   |   |
|---|---|
| Test Type: One-Tailed                       | $\alpha = 0.05$                             |
| $H_0: AI = 1.0$                             | $H_A: AI > 1.0$                             |
| $n = 70$                                    | $\bar{x} = 1.23$                            |
| $\sigma = 0.240$                            | $Z_{\text{crit}} = 1.64$                    |
| Z-Score = 7.93                              |   |
| Result: $Z (7.93) > Z_{\text{crit}} (1.64)$ | Conclusion: Reject $H_0$ in favour of $H_A$ |

**Table 1.** Variables and results of one-tailed hypothesis test of asymmetry index

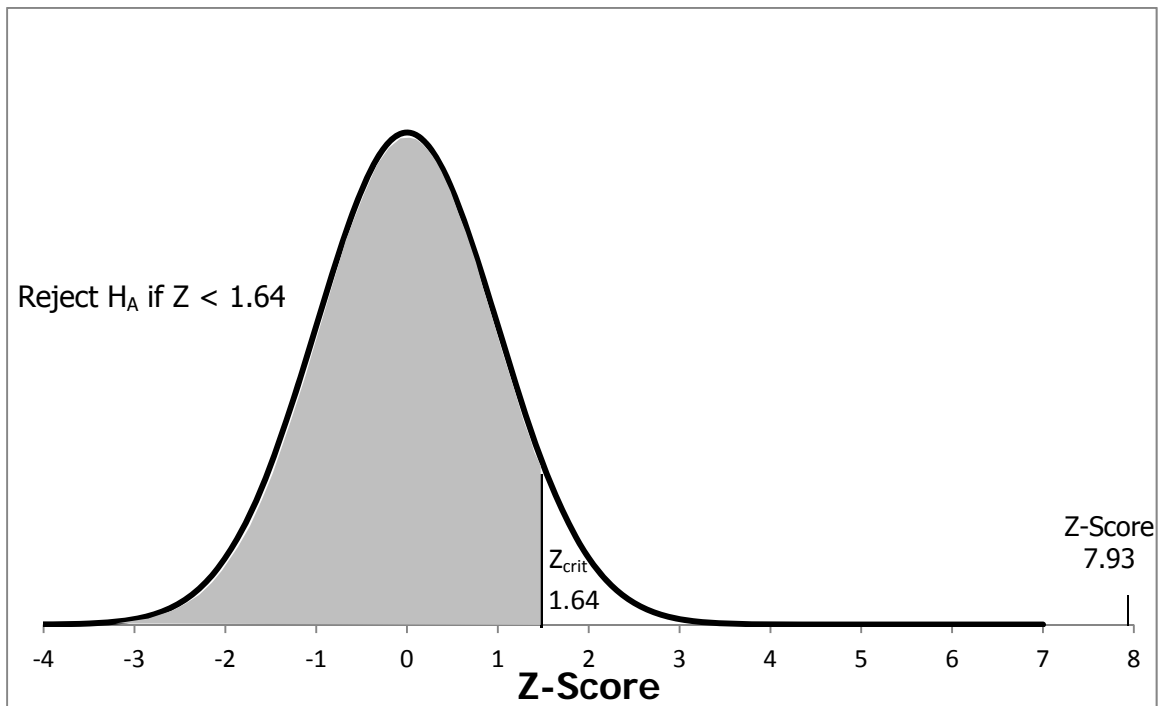


**Figure 18.** AI hypothesis test result graphed under a normal curve.

Alluvial fans selected for this study show that they have longer downstream length profiles than they do upstream. There is a model proposed in section 6.1 of this study that explains this phenomenon, but there is a possible cause of fan asymmetry in the study area that needs to be considered: valley gradient. As shown in Figure 19, if a fan develops on a valley with significant gradient there is potential of deposition from the feeder channel occurring mainly on the downstream side of the fan, because that is the side of the fan that would be downhill. To show that this is not the case with the alluvial fans in this study, valley gradient was calculated and assessed, and shown in the next section.

#### **4.2.1 Valley Gradient**

By initial observation of topographic maps, valley gradient appeared very low. Valley gradient was analyzed to show that fan asymmetry was not the result of sediment deposition on the downhill side of the fan when emerging from a mountain catchment. Valley gradient was calculated by dividing the difference of valley elevation between two contours upstream and downstream from a fan, by the change in elevation between those two contours. The difference of valley elevation ( $D_{VE}$ ) was found by subtracting the upstream contour value ( $C_U$ ) by the downstream contour ( $C_D$ ) shown in Equation 3. Equation 4 is the equation used to find the valley gradient ( $V_G$ ), by dividing the  $D_{VE}$  by the total distance ( $D_T$ ) between the two contours upstream and downstream of the fan, as explained in Section 3.2.1.

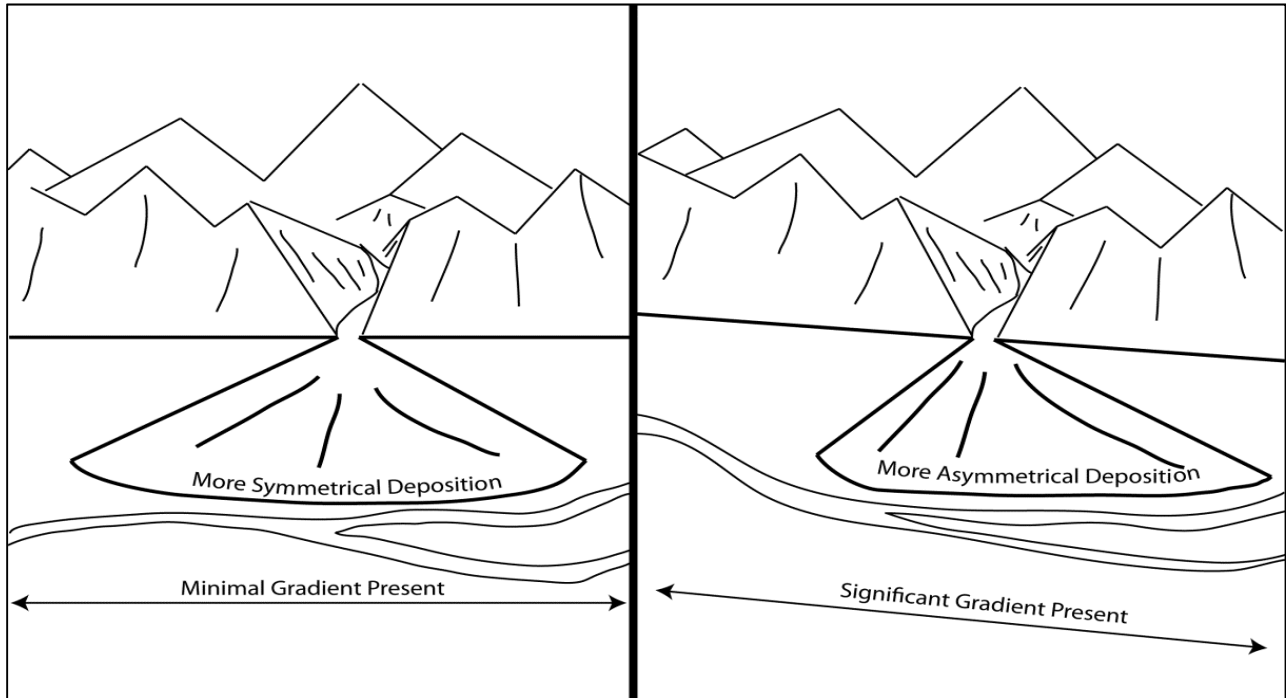


**Figure 19.** *Fan asymmetry can be the result of a fan that develops on a valley that has significant gradient associated with it.*

of valley elevation ( $D_{VE}$ ) was found by subtracting the upstream contour value ( $C_U$ ) by the downstream contour ( $C_D$ ) shown in Equation 3. Equation 4 is the equation used to find the valley gradient ( $V_G$ ), by dividing the  $D_{VE}$  by the total distance ( $D_T$ ) between the two contours upstream and downstream of the fan, as explained in Section 3.2.1.

$$D_{VE} = C_U - C_D$$

**Equation 3.** Difference in Valley Elevation

$$V_G = \frac{D_{VE}}{D_T}$$

**Equation 4.** Valley Gradient Calculation

The results of the valley gradient calculations are shown in Table A3 (in the Appendix). The first column shows gradient in metres of elevation change per metre of distance, and the second column shows the gradient in degrees. The gradient calculations reveal that only two valley sections that alluvial fans have developed on have a gradient greater than 1°, the rest are well under 1°. With such low valley gradients, it is unlikely that alluvial fans within these valleys are asymmetrical because of the deposition on the down valley side of the fan. Valley gradient is concluded to be a negligible factor in the development of asymmetry of alluvial fans.

## CHAPTER 5

### GRADIENT AND STREAM DISTRIBUTION RESULTS AND DISCUSSION

#### 5.1 Alluvial Fan Gradient Calculations and Results

In glaciated regions of the Yukon and Alaska alluvial fans form in wide parabolic-shaped valleys. As discussed in the previous chapter these valleys have such low gradients that the development of fan asymmetry as a result of valley gradient is not likely. If these fans are asymmetrical, and have formed on these valleys; would the fan gradient upstream be the same as the gradient downstream? Since the gradient of the valley on which these alluvial fans have developed is so low and the fans seem to be asymmetrical in distance from apex to toe, the proposed question is interesting. When an asymmetrical fan develops in a valley with low gradient, the distances from apex to toe would be different; one side is longer than the other. The upstream and downstream length profiles are measured from one point that is the same, the apex, and are then measured to different points on the upstream and downstream side. Taking into account that gradient is calculated by the change in elevation over the total distance (similar to Equation 4) (Goudie, 2004), it would make sense that if the gradient for each side was calculated it could be different; because dividing the same change in elevation by different distances would yield different results. Therefore the proposed question relating to a difference in gradient is valid.

The question pertaining to difference of gradient from one side of the fan to the other also relates to the question of fan asymmetry. If one side of the fan is steeper than the other it

would make sense that the distribution of sediment could be unequal. With an unequal distribution of sediment a fan would appear asymmetrical from planform. By answering the question of significant gradient difference between fan sides it could be possible to make a connection between fan asymmetry and difference in gradient.

### 5.1.1 Calculating Fan Gradient

To find the gradient of the upstream and downstream side of each fan, the change in elevation over distance was found. Equation 5 and Equation 6 show the gradient calculation of each side. Each equation was used on every fan to find the upstream gradient ( $U_G$ ) and downstream gradient ( $D_G$ ). Gradient was found by dividing the difference of the apex elevation ( $E_A$ ) and upstream elevation ( $E_U$ ) or downstream elevation ( $E_D$ ), by the upstream length ( $L_U$ ).

$$U_G = \frac{E_U - E_A}{L_U}$$

**Equation 5.** Upstream gradient calculation

$$D_G = \frac{E_D - E_A}{L_U}$$

**Equation 6.** Downstream Gradient calculation

Gradient calculations were performed twice on every fan, once for each side. Even though there was a calculation performed for each side of the fan, the upstream length was always used so that gradient calculations included the same variables on both sides. Since

alluvial fans can have variable deposition on the surface (Blair and McPherson 2009), it is important to use the same length for gradient calculation on each side. For example, if the gradient calculation included the entire lengths from apex to toe from both sides like in the asymmetry index calculation, the side with the longer profile would include parts of the surface face of an alluvial fan that is not measurable on the shorter side. Figure 20 illustrates this problem. If the upstream length profile is represented by A and the downstream length profile is represented by B, there would be a gradient discrepancy because the downstream length profile includes section (A to B) that cannot be measured in the upstream calculation. For comparison purposes the same distance on the fan surface has to be used for the upstream and downstream length profiles. This problem also emphasizes the need for accuracy when taking a measurement of elevation. The measurement point for elevation has to be taken on the surface of the fan at point A, not at the river represented by point B. Figure 20 also illustrates this point. If an elevation measurement is taken at point B instead of point A, there is potential to get a false fan gradient if there is an escarpment (A to B) at the bottom of an alluvial fan.

### 5.1.2 Gradient distribution and hypothesis testing

To plot the gradient distribution, gradient difference (GD) is found for each pair of measurements on all fans. The GD is found by subtracting the upstream gradient ( $U_G$ ) by the downstream gradient ( $D_G$ ). The GD is then plotted on a histogram with a neutral value of 0.0. Any fans with a GD value greater than 0.0 will have a steeper upstream side than downstream side,

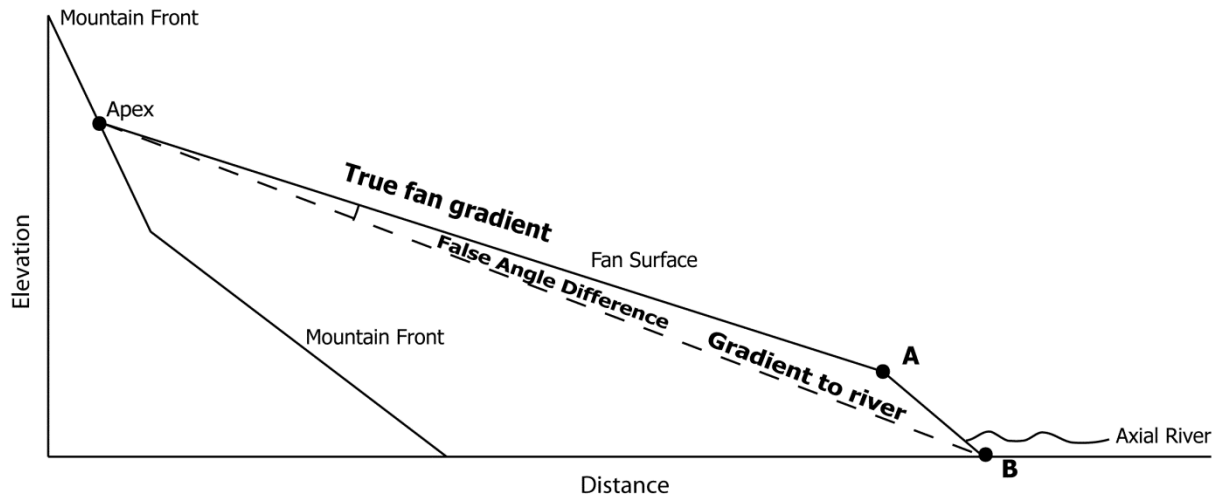


**Figure 20.** *Difference between the true fan gradient and the false fan gradient. To get true fan gradient the elevation has to be recorded at point A. If taken at point B the result of Equation 6 would be false.*

alternatively fans with a GD value less than 0.0 will have steeper downstream sides than upstream sides. Since the gradient hypothesis requires a comparison of two gradients on the same fan, the paired difference experiment will be used to test gradient pairs (McClave and Dietrich 1988). Paired difference experiments can provide more information about the difference between population means than an individual sample experiment (McClave and Dietrich 1988). GD is the difference of each pair, GD of all the sample fans will be averaged and a standard deviation will then be found then used in a two-tailed hypothesis test. The two-tailed paired difference hypothesis test (Equation 7) is similar to a standard two-tailed hypothesis test, but in this case the paired difference is testing the difference of each pair as one population and not testing the pair as two different populations.



$$t - Score = \frac{\bar{x}}{S_{GD} / \sqrt{n_{GD}}}$$

**Equation 7.** t-score statistic for two-tailed paired difference hypothesis test (McClave and Dietrich 1988).

The paired difference experiment two-tailed hypothesis t-score test uses the standard deviation of the difference of the pairs ( $S_{GD}$ ), and the number of differences ( $n_{GD}$ ). A significance level of 0.05 was used, with a null hypothesis that is  $GD = 0$  and the alternative hypothesis is:  $GD \neq 0$ . The null hypothesis supports no significant difference in gradient and the alternative hypothesis supports a difference in gradient between the upstream and downstream side.

### 5.1.3 Fan Gradient Results and Discussion

A two tailed hypothesis test was used in this situation to test the possibility of the upstream side being steeper or gentler than the downstream side. A t-score result greater than 1.64 would mean that the downstream side would be steeper than the upstream side, and if the t-score result is less than -1.64 the upstream gradient would be steeper than the downstream. The results of the paired difference calculation are in Table A2 (in Appendix) which shows that there are many fans that have no difference in gradient (no difference in gradient = 0.000); and the histogram in Figure 21 also shows a 0.000 gradient tendency. The results of the hypothesis test are shown in Table 2 and the results of that test are graphed under a normal curve in Figure 22. Upon initial observation and taking into consideration the mean and standard deviation values from Table 2 it is evident that there was strong frequency

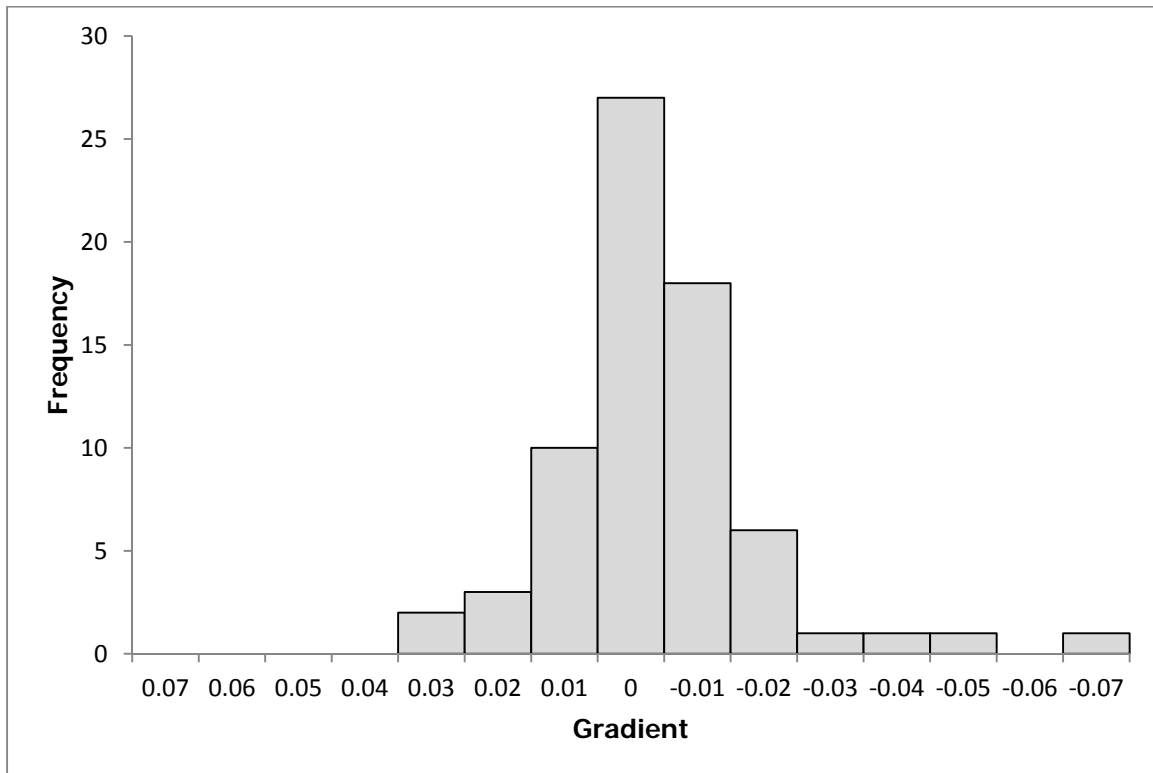


**Figure 21.** *Gradient paired difference histogram*

distribution around 0.0. When the two-tailed hypothesis test was employed to test gradient the resulting t-score fell within the area of rejection, and therefore the alternative hypothesis was rejected in favour of the null. The result of the test rejects the alternate hypothesis which is the idea that there is a significant difference in gradient between the upstream side and downstream side. In summary this indicates that fans in Kluane National Park, Wrangell Mountains and Kenai Mountains have no significant difference in gradient between upstream and downstream sides.

Valley gradient could have an effect on alluvial fan gradient difference as shown in Figure 19. Figure 19 shows that it would make sense to think that if a fan developed on a valley

|  |  |
|--|--|
| Test Type: Two-tailed  | $\alpha = 0.05$                        |
| $H_0: GD = 0$  | $H_A = GD \neq 0$                      |
| $n_{GD} = 70$  | $\bar{x} = -0.001$                     |
| $S_{GD} = 0.240$   | $t_{crit} = -1.64 < \text{and} > 1.64$ |
| t-Score = -0.649   |  |
| Result: $t (-0.649) > t_{crit} (-1.64)$ and $t (-0.649) < t_{crit} (1.64)$ |  |
| Conclusion: Reject $H_A$ in favour of $H_0$                                |  |

**Table 2.** *Variables and results of two-tailed hypothesis test of gradient difference*

with significant gradient the upstream and downstream side of an alluvial fan could have significantly different gradient values. Table A3 (Appendix) shows that valley gradient in all study areas was very minimal; therefore the difference between gradients of the upstream and downstream side would be small or insignificant. Debris flows and sheetfloods would have enough energy to overcome this small gradient and essentially flow “uphill” in a more or less symmetrical shape when emerging from the mountain front. Like fan asymmetry valley gradient is negligible when it comes to fan gradient.

## 5.2. Stream Distribution

The stream distribution hypothesis derives from the question of fan asymmetry; if a fan is asymmetrical, is there a statistical tendency for water to flow down the shortest path to the valley? With that in mind it would be logical to assume that the stream distribution over the

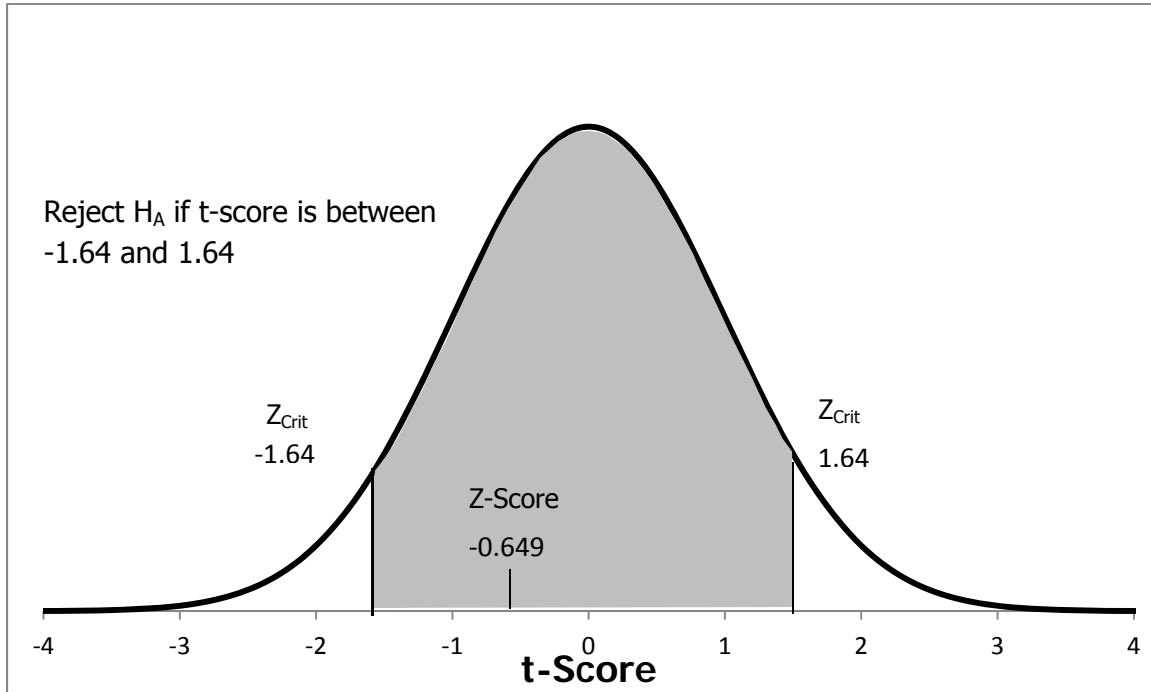


**Figure 22.** Gradient paired difference hypothesis test result graphed under a normal curve

surface of fans could produce a non-random pattern and in turn could correlate with fan asymmetry. Earlier in the study it was shown that fans in Kluane National Park and Alaska are statistically asymmetrical downstream (from apex to toe the downstream side is longer), so when testing stream distribution it is possible that stream distribution may show a statistical tendency towards taking the shorter path down the surface of the fan. This assumption could logically be made because the upstream side is shorter, therefore providing less resistance to a lower point on land. That being said, one has to take into account the possible tendency for the rivers and streams to flow through the other sectors (employed in methodology) so the hypothesis question has to encompass all scenarios. In this case a two-tailed hypothesis test

has to be used to test whether or not the stream distribution on the surface of the fans is non-random.

To find if there is a non-random distribution of surface streams on alluvial fans, a histogram was made consisting of the five sectors from the data collection layout. Each time a stream is found to run through a sector the frequency count will increase by one. Once all 70 fan streams were documented and histogram was made from those results. A two-tailed hypothesis test was performed to test if the stream distribution over the surface is in fact random or not. To review, each fan was divided up into five geometrically equal sectors (described in section 3.2). Sector one is the outer sector of upstream side of the fan and the fifth sector is the outer sector of the downstream side, and sector three is the middle of the fan. Streams can occupy any of those five sectors, so that means, that sector three is the neutral value or the average under a normal curve. The calculation for t-score is shown in Equation 8. The null hypothesis is: stream occupancy (SO) = 3 and the alternative is:  $SO \neq 3$ , with a confidence interval of 0.05.

$$Z = \frac{\bar{x} - 3}{\sigma / \sqrt{n}}$$

**Equation 8.** t-score test for two-tailed hypothesis test of stream distribution (Burt, Barber and Rigby 2009).

### 5.2.1 Stream Distribution Results and Discussion

A histogram of stream distribution is shown in Figure 23 and by examining this histogram it is evident that there is an even stream distribution across all sectors. This

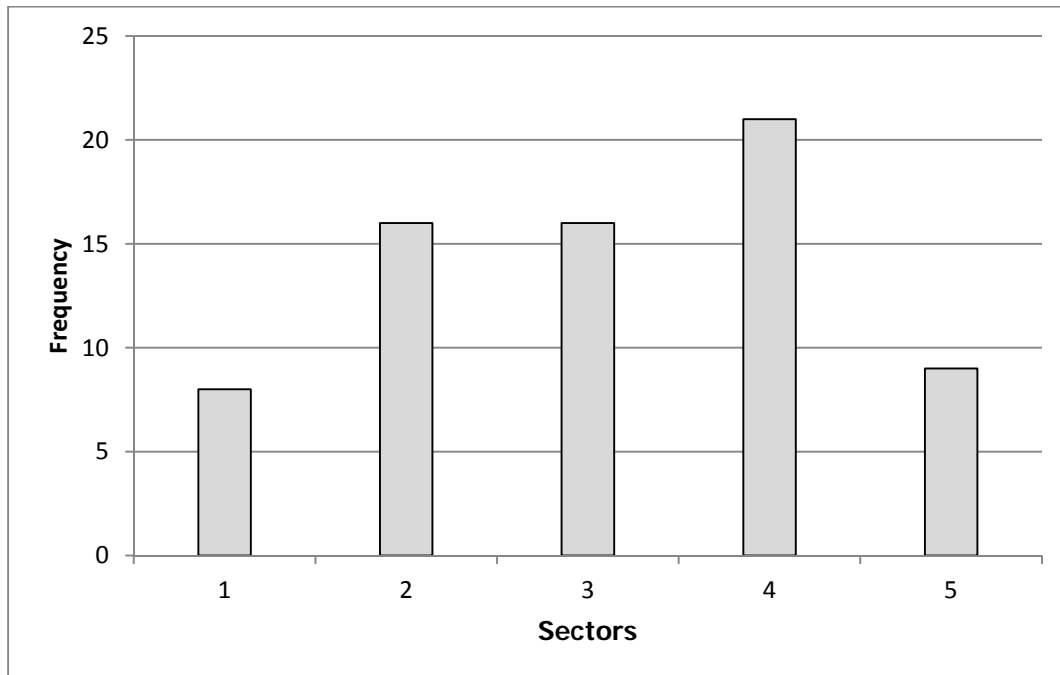


**Figure 23.** *Stream distribution histogram*

observation is supported by the two-tailed hypothesis results show in Figure 24 and Table 3.

For the alternate hypothesis to be supported the t-score had to be greater or less than 1.64 and in this test the z-score was 0.6805 which supported the null hypothesis.

The hypothesis test supported the null hypothesis which in this case was that the stream distribution was close to or equal to stream sector three (the middle sector on the fan, as shown in Figure 16). Since the null hypothesis is supported and the alternative is rejected it is safe to say that there is no statistical tendency for streams to flow down the side of the fan given that the z-score is not above or below 1.64.

|  |   |
|--|---|
| Test Type: Two-Tailed  | $\alpha = 0.05$                               |
| $H_0: SO = 3$  | $H_A = SO \neq 3$                             |
| $n = 70$   | $\bar{x} = 3.1$                               |
| $\sigma = 1.23$  | $Z_{\text{Crit}} = -1.64 < \text{and} > 1.64$ |
| Z-Score = 0.681  |   |
| Result: $Z (0.681) > Z_{\text{Crit}} (-1.64)$ and $< Z_{\text{Crit}} (1.64)$ |   |
| Conclusion: Reject $H_A$ in favour of $H_0$                                  |   |

**Table 3.** *Two tailed stream distribution test breakdown*

In summary, considering the hypothesis test supporting the null hypothesis, and taking into consideration the histogram in Figure 23, it is easy to see that there is a much higher frequency of stream occupancy in the three middle sectors than the outer sectors. This observation does not support the theory that somehow stream distribution and fan asymmetry are linked or that they influence one another, but it does support Blair and McPherson (2004) claim that surface streams are a secondary process and actually degrade the fan. If the surface stream distribution had a tendency towards the downstream side, it would contradict Blair and McPherson theory because the downstream side of the fans in this study area have been aggrading and have longer length profiles than the upstream side.

The central statistical tendency of stream distribution is interesting; upon further observation it became clear that many fans did not have signs of braiding and or anabranching channels on the surface. This can mean that the reduction in flow velocity from the feeder channel to the fan surface was not great enough for the river or stream to start a braiding

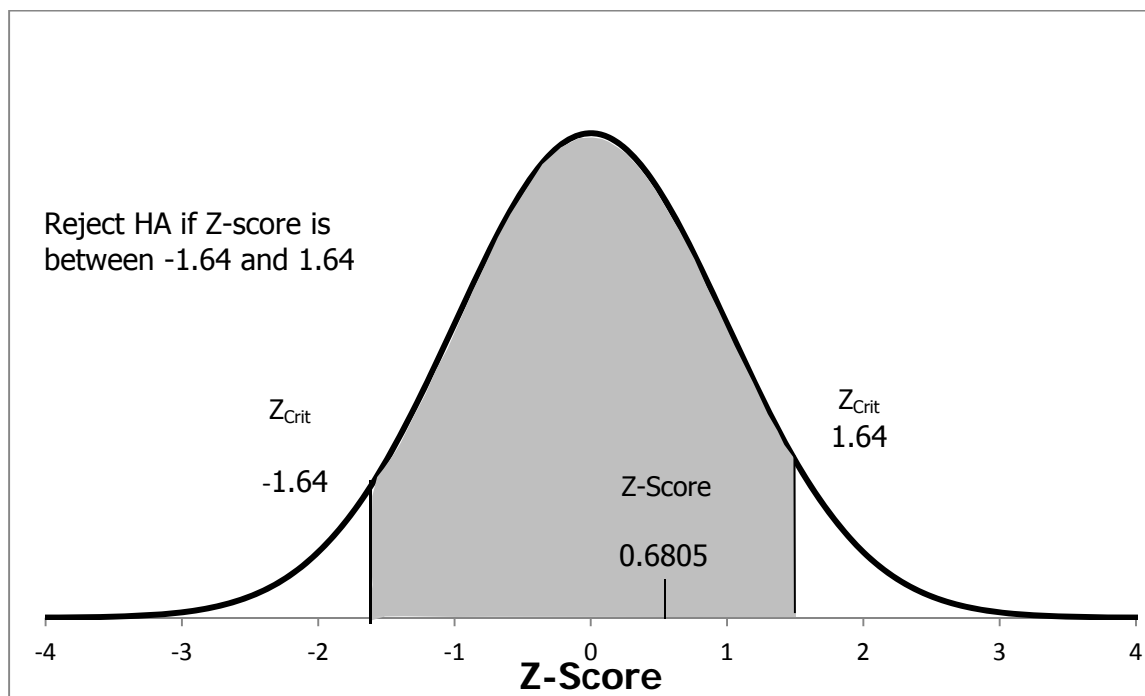


**Figure 24.** *Stream distribution two-tailed hypothesis test results graphed under a normal curve.*

pattern. It could also have been because there was a distinct dissected channel along the surface in which the water is flowing. This could be a reason why there seems to be no connection between stream distribution and asymmetry. A number of fans in this region are very small fans with length profiles that are only a few hundred metres, which means that the difference in gradient from the feeder channel to the fan surface can be minimal and therefore a stream with significant power would continue along its original path even over the fan surface.



## CHAPTER 6

### DISCUSSION AND CONCLUSIONS

#### 6.1 Cumulative Discussion

This study's primary research question derived from the idea that alluvial fans could have a statistical difference in lengths from apex to toe when comparing the length profiles of the upstream side and the downstream side in plan perspective. With that in mind it was purposed that fans in Kluane National Park and Alaska could have statistically different length profiles when comparing the upstream and downstream sides. It was also purposed that if the selected fans showed a statistical asymmetrical tendency, there could be a difference in fan surface gradient between the aforementioned sides as well. Finally, a third proposition addressed whether there could be a connection between fan asymmetry and surface stream distribution. The results of the fan asymmetry hypothesis test definitively supported the alternate hypothesis, and showed that fans in this study have a statistically longer downstream profile than an upstream profile, and are therefore asymmetrical. As mentioned in previous chapters the results of the difference in gradient test and surface stream distribution test provided no evidence that supported a correlation between those phenomena and that of fan asymmetry.

The gradient or slope on an alluvial fan depends on a number of factors such as catchment area, clast size of composition, and climatic affects (Bull, 1962; Hooke 1968 and Blair and McPherson, 2004). The gradient of an alluvial fan could affect where the sediment supplied

by the feeder channel will deposit, so if there is a difference in gradient from one side of a fan to the other it could explain why there is asymmetry. In this case there is no statistical difference in gradient within fans in this study, so asymmetry has to be caused by another process. Fan asymmetry has been already shown not to cause a difference in gradient in this study, but an interesting question is: How do fans become asymmetrical?

If asymmetry was not a result of a difference in gradient of the valley on which a fan develops or the difference in gradient between the upstream and downstream sides, how is there a statistical downstream asymmetry present in these fans? The answer seems to lie within a commonality between the selected fans of Kluane National Park, Wrangell Mountains and Kanai Mountains. This commonality is the presence of an axial river within the valley in which these fans have developed. It appears that axial rivers have been eroding the toes of these fans or as Leeder and Mack (2001) have called this process, 'toe-cutting.' This process affects the toe of an alluvial fan by removing sediment and transporting it downstream. Leeder and Mack illustrate and describe 'toe-cutting' as the straightening of the toe of the fan. There is a difference between Leeder and Mack's 'toe-cutting' theory and the 'toe-cutting' theory presented in this study. 'Toe-cutting' in this study is occurring primarily on the upstream side as illustrated in Figure 25B. This upstream 'toe-cutting' restricts fan development upstream because all aggradation on that side of the fan is quickly eroded away.

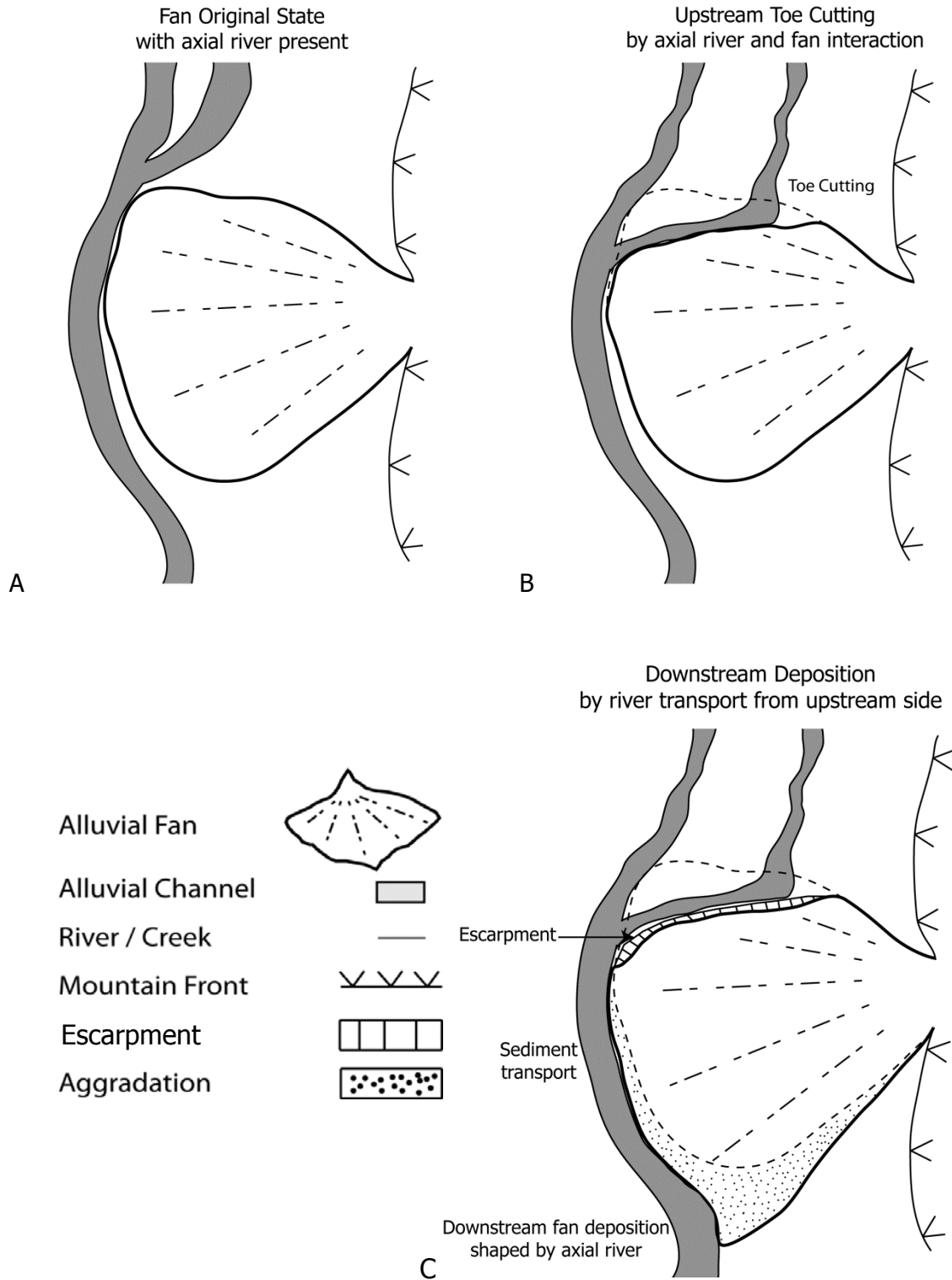


**Figure 25.** Initial stages of alluvial fan asymmetry development. Fans go from their original state and become eroded on the upstream side by an axial river.

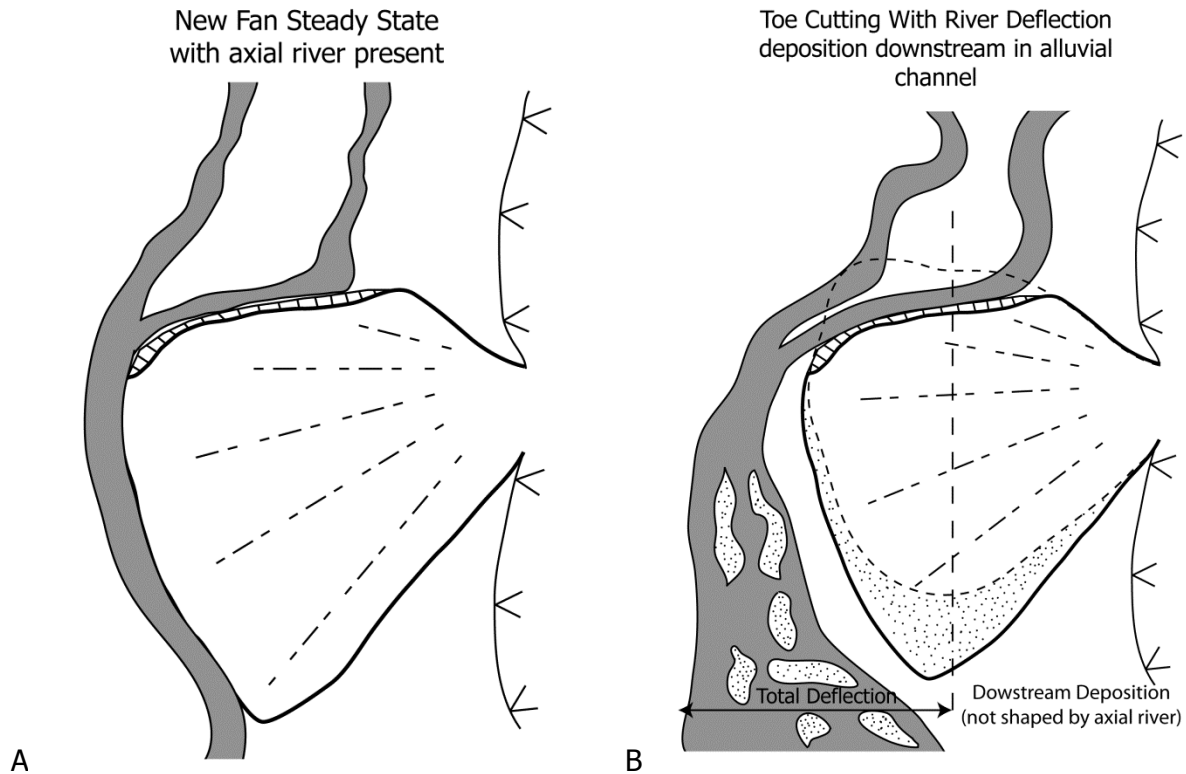
Erosion of the upstream side of alluvial fans within this study area creates asymmetry, as shown in Figure 25C. As the axial river erodes the upstream side of an alluvial fan the sediment becomes entrained by the river and is transported downstream and contributes to the alluvial channel load. Figure 25 and Figure 26 are the proposed stages an alluvial fan goes through to become asymmetrical.

Figure 25A illustrates a fan that has developed over time in a glaciated valley by processes that are discussed in section 1.4, without the interaction between it and the axial river for a significant period of time. Interaction of an axial stream and a fan toe occurs when the river within a glaciated valley migrates and interacts with the alluvial fan. This interaction can occur soon after an alluvial fan has developed or many years after. Once interaction with the toe of an alluvial fan is underway the river begins to erode the upstream side of the fan shown in Figure 25B. As a river continues to erode the upstream side of an alluvial fan it will transport the sediment taken from the fan downstream. If there is limited space between the alluvial fan and the mountain front opposite the alluvial fan the river will continue to follow the fan toe and shape the downstream side. If there is adequate room between the alluvial fan and the opposite mountain front the river may be deflected away from the fan and sediment will be carried down the alluvial channel as illustrated in Figure 26B.

The 'toe-cutting' erosional process is continuous as long as there is interaction between an alluvial fan toe and an axial river; therefore, the fan will fall into an asymmetrical steady state as shown in Figure 26A. At this point any aggradation upstream will be quickly eroded

away and the fan will stay asymmetrical in planform until the river migrates away from said fan; at that time the fan will return to the initial state conceived in Figure 25A.

The results and methods of this study provide some of the first insight into alluvial fan asymmetry. Alluvial fan asymmetry in this study is the result of a combination of primary and secondary processes. This suggests that the secondary process of toe-cutting erodes the upstream side of a fan and primary processes enlarge the downstream side and increase the asymmetry index. The idea of fan asymmetry has been presented in articles such as Leeder and Mack (2001) and Hashimoto (2008), but the idea has never been fully investigated. This study uses basic geomorphological principles regarding alluvial fan development and morphometry, and also integrates similar ideas highlighted in other research to describe fan asymmetry. There are still many questions to be asked when it comes to alluvial fan asymmetry. Questions like: Does alluvial fan asymmetry exist without the presence of an axial river? This work can be the building block for new studies concerning alluvial fan asymmetry in planform. Hopefully, future researchers can build on ideas presented here and develop a more refined process of studying alluvial fan asymmetry, and in turn increase the depth of knowledge on the subject.



**Figure 26.** (A) After erosion starts fans enter a "steady" asymmetrical state with the axial river shaping the toe or (B) a fan will enter a "steady" asymmetrical state while deflecting the axial river away from the toe downstream.

## 6.2 Conclusions

Analysis of the selected alluvial fans in Kluane National Park, Wrangell Mountains and the Kenai Mountains reveals that fans in these study areas are statistically asymmetrical. The fans within these study areas are statistically asymmetrical, yet they are not asymmetrical as a result of a difference in gradient between the upstream and downstream sides. The results of the paired hypothesis test of gradient difference showed no statistical difference in gradient between the upstream and downstream sides. With no statistical difference in gradient present it also follows sense that stream distribution resulted in a random distribution as well, because there is not enough difference in gradient for water to flow down the 'steepest path,' so the

water spreads over the surface of a fan because of similar gradient across the face. This study reveals that fan asymmetry is statistically significant and is not a product of the differences in fan gradient or from non-random stream distribution.

Fan asymmetry in this study seems to be the result of axial river erosion by a process called 'toe-cutting,' affecting the upstream side of the alluvial fans in this study area. As the axial river interacts with an alluvial fan along its toe upstream, the flowing water erodes away the upstream side and transports the sediment downstream. As primary processes enlarge the fan the axial river (by means of 'toe cutting'; a secondary process) quickly removes the sediment preventing an alluvial fan from developing upstream, creating asymmetry. The processes and stages highlighted in this study that create fan asymmetry will not necessarily be the case if asymmetry is found in alluvial fans in another region, but the methodology employed in this study provides a viable way to find fan asymmetry.

With the application of topographic maps and Google Earth this research project has provided the tools to analyze fan asymmetry, applicable to fans in all regions with adequate data. With the sparse mention of fan asymmetry in published literature this research project can be the starting point of future research into the asymmetry of alluvial fans.

## REFERENCE LIST

- Ahnert, F., 1970. Functional relationships between denudation, relief, and uplift in large mid-latitude drainage basins. *American Journal of Science*, vol. 268: 243-263.
- Al-Farraj, A., and Harvey, A.M., 2000. Desert pavement characteristics on wadi terrace and alluvial fan surfaces: Wadi Al-Bih, U.A.E. and Oman. *Geomorphology*, vol. 35: 279-297.
- Beaudoin, A.B., and King, R.H., 1994. Holocene palaeoenvironmental record preserved in a paraglacial alluvial fan, Sunwapta Pass, Jasper National Park, Alberta, Canada. *CATENA*, vol. 22:227-246.
- Blair, T.C., 1987. Tectonic and hydrologic controls on cyclic alluvial fan, fluvial, and lacustrine rift-basin sedimentation, Jurassic-lowermost Cretaceous Todos Santos Formation, Chiapas, Mexico. *Journal of Sedimentary Petrology*, vol. 57: 845-862.
- Blair, T.C., and McPherson, J.G. 1994. Alluvial Fan processes and forms. *Geomorphology of Desert Environments* (eds A.D. Abrahams and A.J. Parsons). Chapman and Hall, London, pp. 354-402.
- Blair, T.C., and McPherson, J.G. 2009. Processes and forms of alluvial fans. In *Geomorphology of Desert Environments*, 2<sup>nd</sup> ed. Edited by A.J. Parsons, A.D. Abrahams. Springer Science+Business Media. pp. 413-459.
- Bull, W.B., 1977. The Alluvial Fan Environment. *Progress in Physical Geography*, vol. 1: 222-270.
- Bull, W.B., 1979. The threshold of critical power in streams. *Geological Society of America Bulletin*. vol. 90: 453-464.
- Burt, J.E., Barber, G.M., Rigby, D.L., 2009. Elementary Statistics for Geographers. 3<sup>rd</sup> ed. The Guilford Press.
- Calvache, M.L., Viseras, C., and Fernandez, J. 1997. Controls of fan development – evidence from fan morphometry and sedimentology: Sierra Nevada, Spain. *Geomorphology*, vol. 21: 69-84.
- Campbell, C., 1998. Postglacial evolution of a fine-grained alluvial fan in the northern Great Plains, Canada. *Palaeogeography, Palaeoclimatology, Palaeoecology*, vol. 139: 233-249.
- Chakraborty, T., and Ghosh, P., 2010. The geomorphology and sedimentology of the Tista megafan, Darjeeling Himalaya; Implications for megafan building processes. *Geomorphology*, vol. 115: 252-266.
- Chiverrell, R.C., Harvey, A.M., and Foster, G.C., 2007. Hillslope gullying in the Solway Firth-Morecambe Bay region, Great Britain: responses to human impact and/or climatic deterioration? *Geomorphology*, vol. 84: 317-343.



- DeGraff, J.V., 1994. The geomorphology of some debris flows in the southern Sierra Nevada, California. *Geomorphology*, vol. 10: 231-252.
- Derbyshire, E. and Owen, L.A. 1990. Quaternary alluvial fans in the Karakoram Mountains. *Alluvial Fans: A Field Approach* (eds A.H. Rachocki and M. Church). John Wiley and Sons Ltd, Chichester.
- Environment Canada, 2009. Canadian Climate Normals or Averages 1971–2000. [http://www.climate.weatheroffice.ec.gc.ca/climate\\_normals/index\\_e.html](http://www.climate.weatheroffice.ec.gc.ca/climate_normals/index_e.html).
- Florsheim, J.L., 2004. Side-valley tributary fans in high-energy river floodplain environments: sediment sources and depositional processes, Navarro River basin, California. *Geological Society of America Bulletin*, vol. 116: 923-937.
- Gabris, G., and Nagy, B., 2005. Climate and tectonically controlled river style changes on the Sajo-Hernad alluvial fan (Hungary). *Alluvial Fans: geomorphology, sedimentology, dynamics*. Geological Society Special Publication, vol. 251: 61-67.
- Gardener, T.W, Webb, J., Davis, A.G, Cassel, E.J., Pezzia, C., Merritts, D.J., and Smith, B., 2006. Late Pleistocene landscape response to climate change; eolian and alluvial fan deposition, Cape Liptrap, southeastern Australia. *Quaternary Science Reviews*, vol. 25: 1552-1569.
- Gohain, K., and Parkash, B., 1990. Morphology of the Kosi megafan. *Alluvial Fans: A Field Approach* (eds A.H. Rachocki and M. Church). John Wiley and Sons, Ltd, Chichester, pp. 151-178.
- Google Earth V 6.2.2.6613. (July 30, 2007). Yukon, Canada. 60° 49' 21.41"S, 138° 24' 43.58"W,. DigitalGlobe 2012. March 14, 2013.
- Goudie, A.S., 2004. *Encyclopaedia of Geomorphology*. Vol 2. London and New York: Routledge.
- Gomez-Villar, A., and Garcia-Ruiz, J.M., 2000. Surface sediment characteristics and present dynamics in alluvial fans of the central Spanish Pyrenees. *Geomorphology*, vol. 34; 127-144.
- Harvey, A.M., 1984. Debris Flows and fluvial deposits in Spanish Quaternary alluvial fans: implications for fan morphology. *Sedimentology of Gravels and Conglomerates* (eds E.H. Koster and R. Steel), Canadian Society of Petroleum Geologists, Memoir, vol. 10: pp. 23-132.
- Harvey, A.M., 1987. Alluvial fan dissection: relationships between morphology and sedimentation. Desert Sediments, Ancient and modern (eds L. Frostick and I. Reid). *Geological Society of London, Special Publication*, vol. 35; pp. 87-103.
- Harvey, A.M., 1990. Factors influencing Quaternary fan development in southeast Spain. *Alluvial Fans: A Field Approach* (eds A.H. Rachocki and M. Church). Wiley, New York, pp. 247-270.
- Harvey, A.M., 2002. The relationships between alluvial fans and fan channels within Mediterranean mountain fluvial systems. *Dryland Rivers: Hydrology and Geomorphology of Semi-arid Channels* (eds L. Bull and M.J. Kirkby), John Wiley and Sons Ltd. pp. 205-226.

- Harvey, A.M., 2010. *Sediment Cascades: An Integrated Approach* (eds T. Burt and R. Allison), John Wiley and Sons Ltd. pp. 156-179.
- Harvey, A.M., 2011. *Arid Zone Geomorphology: Process, Form and Change in Drylands*, 3<sup>rd</sup> ed. John Wiley and Sons, Ltd.
- Hashimoto, A., Oguchi, T., and Hayakawa, Y., Lin, Z., Saito, K., Wasklewicz, A.T., 2008. GIS analysis of depositional slope change at alluvial-fan toes in Japan and the American Southwest. *Geomorphology*, vol. 100: 120-130.
- Haug, E.W., Kraal, E.R., Sewall, J.O., Van Dijk, M., Diaz, C.G., 2010. Climatic and geomorphic interactions on alluvial fans in the Atacama Desert, Chile. *Geomorphology*, vol. 121: 184-196.
- Houston, J., 2002. Groundwater recharge through an alluvial fan in the Atacama Desert, northern Chile: mechanisms, magnitudes of causes. *Hydrological Processes*, vol. 16: 3019-3035.
- Huggett, J.R., 2011. *Fundamentals of Geomorphology*, 3<sup>rd</sup> ed. London: Routledge.
- Jackson, L.E., and Clague, J.J., 1991. The Cordilleran Ice Sheet: One Hundred and Fifty Years of Exploration and Discovery. *Géographie physique et Quaternaire*, vol. 45: 269-280.
- Jervey, M.T., 1988. Quantitative geological modelling of siliciclastic rock sequences and their seismic expression. In: Wilgus, C.K., Hastings, B.S., Kendall, C.G.St.C., Posamentier, H.W., Ross, C.A., Van
- Kesel, R.H., and Spicer, B.E., 1985. Geomorphic relationships and ages of soils on alluvial fans in the Rio General Valley Costa Rica. *Catena*, vol. 12: 149-166.
- Wagoner, J.C. (Eds.), *Sea Level Changes: An Integrated Approach*. Society of Paleontologists and Mineralogists, Special Publication, vol. 42. SEPM, Tulsa, pp. 47-69.
- Leeder, M.R., and Mack, G.H., 2001. Lateral erosion ('toe-cutting') of alluvial fans by axial rivers: implications for analysis and architecture. *Journal of the Geological Society, London*, vol. 158; 885-893.
- Levson, V.M., and Rutter, N.W., 2000. Influence of bedrock geology on sedimentation in Pre-Late Wisconsinan alluvial fans in the Canadian Rocky Mountains. *Quaternary International*, vol. 68-71: 133-146.
- McClave, J.T., and Dietrich, F.H., 1988. *Statistics*. 4<sup>th</sup> ed. Collier Macmillan Canada Inc.
- McArthur, J.L., 1987. The characteristics, classification and origin of Late Pleistocene fan deposits in the Cass Basin, Canterbury, New Zealand. *Sedimentology*, vol. 34: 459-471.
- Miall, A.D., 1996. *The Geology of Fluvial Deposits: Sedimentary Facies, Basin Analysis and Petroleum Geology*. Springer-Verlag, Berlin, pp. 582.

- Muhs, R.D., McGeehin, J.P., Beann, J., and Fisher, E., 2004. Holocene loess deposition and soil formation as competing processes Matanuska Valley, southern Alaska. *Quaternary Research*, vol. 61: 265-276.
- Nicholas, A.P., Clarke, L., and Quine, T.A., 2009. A numerical modelling and experimental study of flow width dynamics on alluvial fans. *Earth Surface and Landforms*. vol. 34: 527-530.
- Nicholas, D.R., 1958. Engineering Geologic Map of the Southeastern Copper River Basin, Alaska. Interior –Geological Survey, Washington.
- Patton, P.C., 1988. Drainage basin morphometry and floods. *Flood geomorphology*. Wiley, New York, pp. 51-64.
- Plummer, C.C., Carlson, D.H., McGeary, D., Eyles, C., and Eyles, N., 2007. *Physical Geology and the Environment*. 2<sup>nd</sup> ed. McGraw-Hill Ryerson. pp. 373.
- Posamentier, H.W., and Vail.R., 1988. Eustatic control on clastic depositions: II. Sequence and systems tracts models. Sea Level Changes: And Integrated Approach. *Society of Economics Paleontologists and Mineralogists, Special Publication*, vol. 42. SEPM, Tulsa, pp. 125-154.
- Rickenmann, D., and Zimmerman, M., 1993. The 1987 debris flows in Switzerland: documentation and analysis. *Geomorphology*, vol. 8: 175-189.
- Ritter, D.F., and Ten Brink, N.W. 1986. Alluvial Fan Development and the Glacial-Glaciofluvial Cycle, Nenana Valley, Alaska. *Journal of Geology*, vol. 94: 617-625.
- Saito, K., and Oguchi, T., 2005. Slope of alluvial fans in humid regions of Japan, Taiwan and the Philippines. *Geomorphology*, vol. 70: 147-162.
- Sancho, C., Pena, J.L., Rivelli, F., Rhodes, E., Munoz, A., 2008. Geomorphological evolution of the Tilcara alluvial fan (Jujuy Province, NW Argentina): Tectonic implications and palaeoenvironmental considerations. *Journal of South American Earth Sciences*, vol. 25: 68-77.
- Schuum, S.A., 1963. The disparity between the present rates of denudation and orogeny. *U.S. Survey Professional Paper*, 454-H.
- Schuum, S.A., 1977. *The Fluvial System*. Wiley, New York.
- Silva, P.G., Harvey, A.M., Zazo, C., and Goy, J.L., 1992. Geomorphology, depositional style and morphometric relationships of Quaternary alluvial fans in the Guadalentin depression (Murcia, southeast Spain). *Zeitschrift fur Geomorphologie* N.F. 36, 325–341.
- Tanarro, L.M., and Munoz, J., 2012. Rockfalls in the Duraton canyon, central Spain: Inventory and statistical analysis. *Geomorphology*, vol. 169-170: 17-29.
- Viseras, C., Calvache, M.L., Soria, J.M., and Fernandez, J., 2003. Differentail features of alluvial fans controlled by tectonic or eustatic accomodation space. Examples from the Betic Cordillera, Spain. *Geomorphology*. vol. 50: 181-202.

- Wahl, H.E., D.B. Fraser, R.C. Harvey, and J.B. Maxwell. 1987. Climate of Yukon. Climatological Studies Number 40. Atmospheric Environment Service, Environment Canada. Pp. 233.
- Ward, B.C., Bond, J.D., and Grosse, J.C., 2007. Evidence for a 55-50 ka (early Wisconsin) glaciation of the Cordilleran ice sheet, Yukon Territory, Canada. *Quaternary Research*, vol. 68; 141-150.
- Wells, S.G., and Harvey, A.M. 1987. Sedimentologists and geomorphic variations in storm generated alluvial fans. *Geological Society of America Bulletin*, vol. 98: 182-198.
- Williams, G.E., 1973. Late Quaternary piedmont sedimentation, soil formation and palaeoclimates in arid South Australia. *Zeitschrift fur Geomorphologie*, vol. 17: 102-125.

**APPENDIX**

**Table A1.** Data from data collection layout

| Fan Code       | Lengths (m)    |                |      | Elevations (m) |            | Change in Elevation (m) |            | Stream Sector | Asymmetry Index |
|----------------|----------------|----------------|------|----------------|------------|-------------------------|------------|---------------|-----------------|
|                | L <sub>U</sub> | L <sub>D</sub> | Apex | Upstream       | Downstream | Upstream                | Downstream |               |                 |
| <b>A-CH-01</b> | 1456           | 2315           | 483  | 456            | 450        | 27                      | 33         | 2             | 1.59            |
| <b>A-CH-02</b> | 2297           | 3332           | 475  | 420            | 431        | 55                      | 44         | 2             | 1.45            |
| <b>A-CH-03</b> | 2903           | 3972           | 425  | 375            | 390        | 50                      | 35         | 3             | 1.37            |
| <b>A-CH-04</b> | 1055           | 1217           | 485  | 383            | 394        | 102                     | 91         | 2             | 1.15            |
| <b>A-CH-05</b> | 2158           | 1833           | 359  | 231            | 222        | 128                     | 137        | 3             | 0.85            |
| <b>A-CH-06</b> | 1198           | 1509           | 170  | 168            | 169        | 2                       | 1          | 2             | 1.26            |
| <b>A-CI-01</b> | 652            | 952            | 754  | 715            | 711        | 39                      | 43         | 5             | 1.46            |
| <b>A-CI-02</b> | 916            | 1048           | 832  | 670            | 656        | 162                     | 176        | 5             | 1.14            |
| <b>A-CI-03</b> | 1146           | 1549           | 669  | 613            | 610        | 56                      | 59         | 1             | 1.35            |
| <b>A-CI-04</b> | 1675           | 1613           | 503  | 382            | 358        | 121                     | 145        | 5             | 0.96            |
| <b>A-CI-05</b> | 789            | 760            | 435  | 369            | 367        | 66                      | 68         | 2             | 0.96            |
| <b>A-CO-01</b> | 936            | 1669           | 89   | 85             | 85         | 4                       | 4          | 3             | 1.78            |
| <b>A-CO-02</b> | 862            | 978            | 279  | 107            | 91         | 172                     | 188        | 2             | 1.13            |
| <b>A-CO-03</b> | 866            | 878            | 124  | 96             | 106        | 28                      | 18         | 4             | 1.01            |
| <b>A-CO-04</b> | 251            | 402            | 120  | 108            | 109        | 12                      | 11         | 3             | 1.60            |
| <b>A-RO-01</b> | 1258           | 1561           | 768  | 634            | 636        | 134                     | 132        | 4             | 1.24            |
| <b>A-RO-02</b> | 1154           | 1506           | 657  | 627            | 627        | 30                      | 30         | 5             | 1.31            |
| <b>A-RO-03</b> | 931            | 926            | 783  | 633            | 631        | 150                     | 152        | 2             | 0.99            |
| <b>A-SK-01</b> | 608            | 599            | 803  | 723            | 715        | 80                      | 88         | 1             | 0.99            |

Table A1 (Continued)

| Fan Code | Lengths (m)    |                | Apex | Elevations (m) |            | Change in Elevation (m) |            | Stream Sector | Asymmetry Index |
|----------|----------------|----------------|------|----------------|------------|-------------------------|------------|---------------|-----------------|
|          | L <sub>U</sub> | L <sub>D</sub> |      | Upstream       | Downstream | Upstream                | Downstream |               |                 |
| A-SK-02  | 626            | 785            | 808  | 712            | 720        | 96                      | 88         | 3             | 1.25            |
| A-SK-03  | 1312           | 1368           | 637  | 540            | 544        | 97                      | 93         | 4             | 1.04            |
| A-SK-04  | 687            | 753            | 585  | 519            | 500        | 66                      | 85         | 1             | 1.10            |
| A-ST-01  | 647            | 883            | 1119 | 1094           | 1094       | 25                      | 25         | 5             | 1.36            |
| A-ST-02  | 860            | 1334           | 1097 | 1086           | 1071       | 11                      | 26         | 4             | 1.55            |
| A-ST-03  | 791            | 796            | 1063 | 1034           | 1026       | 29                      | 37         | 5             | 1.01            |
| A-ST-04  | 758            | 925            | 1119 | 1030           | 1031       | 89                      | 88         | 5             | 1.22            |
| A-ST-05  | 1217           | 1412           | 1123 | 1023           | 1014       | 100                     | 109        | 4             | 1.16            |
| A-ST-06  | 697            | 1005           | 1125 | 1007           | 1008       | 118                     | 117        | 1             | 1.44            |
| A-WR-01  | 1344           | 1418           | 787  | 684            | 678        | 103                     | 109        | 2             | 1.06            |
| A-WR-02  | 1069           | 1134           | 861  | 674            | 673        | 187                     | 188        | 4             | 1.06            |
| A-WR-03  | 717            | 904            | 723  | 618            | 611        | 105                     | 112        | 4             | 1.26            |
| A-WR-04  | 1227           | 1178           | 800  | 632            | 612        | 168                     | 188        | 4             | 0.96            |
| Y-AL-01  | 97             | 117            | 595  | 593            | 591        | 2                       | 4          | 3             | 1.21            |
| Y-AL-02  | 559            | 735            | 549  | 514            | 517        | 35                      | 32         | 1             | 1.31            |
| Y-AL-03  | 416            | 445            | 570  | 534            | 520        | 36                      | 50         | 3             | 1.07            |
| Y-AL-04  | 421            | 618            | 552  | 525            | 525        | 27                      | 27         | 3             | 1.47            |
| Y-AL-05  | 576            | 734            | 561  | 529            | 534        | 32                      | 27         | 1             | 1.27            |
| Y-AL-06  | 325            | 380            | 513  | 474            | 475        | 39                      | 38         | 3             | 1.17            |

Table A1 (Continued)

| Fan Code | Lengths (m)    |                |      | Elevations (m) |            | Change in Elevation (m) |            | Stream Sector | Asymmetry Index |
|----------|----------------|----------------|------|----------------|------------|-------------------------|------------|---------------|-----------------|
|          | L <sub>U</sub> | L <sub>D</sub> | Apex | Upstream       | Downstream | Upstream                | Downstream |               |                 |
| Y-AL-07  | 290            | 422            | 482  | 481            | 481        | 1                       | 1          | 4             | 1.46            |
| Y-DI-01  | 549            | 598            | 1080 | 1026           | 1015       | 54                      | 65         | 4             | 1.09            |
| Y-DI-02  | 356            | 433            | 1071 | 964            | 972        | 107                     | 99         | 4             | 1.22            |
| Y-DI-03  | 511            | 798            | 991  | 922            | 939        | 69                      | 52         | 3             | 1.56            |
| Y-DO-01  | 2332           | 3977           | 987  | 924            | 942        | 63                      | 45         | 3             | 1.71            |
| Y-DO-02  | 1218           | 1152           | 1020 | 944            | 933        | 76                      | 87         | 2             | 0.95            |
| Y-DO-03  | 841            | 1039           | 1114 | 947            | 931        | 167                     | 183        | 3             | 1.24            |
| Y-DO-04  | 3703           | 7271           | 926  | 899            | 887        | 27                      | 39         | 3             | 1.96            |
| Y-DO-05  | 2564           | 3550           | 910  | 844            | 840        | 66                      | 70         | 2             | 1.38            |
| Y-DO-06  | 2688           | 3448           | 808  | 769            | 799        | 39                      | 9          | 2             | 1.28            |
| Y-DU-01  | 1330           | 1637           | 786  | 710            | 703        | 76                      | 83         | 4             | 1.23            |
| Y-DU-02  | 905            | 1246           | 686  | 666            | 649        | 20                      | 37         | 4             | 1.38            |
| Y-DU-03  | 349            | 496            | 709  | 638            | 661        | 71                      | 48         | 2             | 1.42            |
| Y-DU-04  | 956            | 1242           | 682  | 626            | 624        | 56                      | 58         | 4             | 1.30            |
| Y-KA-01  | 938            | 958            | 860  | 741            | 737        | 119                     | 123        | 5             | 1.02            |
| Y-KA-02  | 1917           | 2306           | 874  | 728            | 732        | 146                     | 142        | 4             | 1.20            |
| Y-KA-03  | 1363           | 1556           | 800  | 690            | 681        | 110                     | 119        | 1             | 1.14            |
| Y-KA-04  | 1635           | 2994           | 704  | 665            | 670        | 39                      | 34         | 4             | 1.83            |
| Y-KA-05  | 1087           | 944            | 738  | 661            | 667        | 77                      | 71         | 2             | 0.87            |



Table A1 (Continued)

| Fan Code | Lengths (m)    |                | Elevations (m) |          | Change in Elevation (m) |          | Stream Sector | Asymmetry Index |            |
|----------|----------------|----------------|----------------|----------|-------------------------|----------|---------------|-----------------|------------|
|          | L <sub>U</sub> | L <sub>D</sub> | Apex           | Upstream | Downstream              | Upstream |               |                 | Downstream |
| Y-KA-06  | 1000           | 1052           | 715            | 620      | 630                     | 95       | 85            | 4               | 1.05       |
| Y-KA-07  | 604            | 688            | 716            | 646      | 671                     | 70       | 45            | 2               | 1.14       |
| Y-KA-08  | 225            | 339            | 667            | 632      | 632                     | 35       | 35            | 4               | 1.51       |
| Y-KA-09  | 426            | 413            | 694            | 627      | 630                     | 67       | 64            | 3               | 0.97       |
| Y-KA-10  | 422            | 488            | 695            | 627      | 629                     | 68       | 66            | 3               | 1.16       |
| Y-SL-01  | 1136           | 1096           | 933            | 796      | 800                     | 137      | 133           | 2               | 0.96       |
| Y-SL-02  | 535            | 586            | 865            | 785      | 793                     | 80       | 72            | 4               | 1.10       |
| Y-SL-03  | 792            | 803            | 880            | 785      | 761                     | 95       | 119           | 4               | 0.99       |
| Y-SL-04  | 661            | 492            | 874            | 783      | 776                     | 91       | 98            | 1               | 0.74       |
| Y-SL-05  | 818            | 961            | 862            | 776      | 769                     | 86       | 93            | 4               | 1.17       |
| Y-SL-06  | 942            | 1003           | 924            | 800      | 798                     | 124      | 126           | 5               | 1.06       |
| Y-SL-07  | 2472           | 3006           | 827            | 787      | 766                     | 40       | 61            | 2               | 1.22       |
| Y-SL-08  | 2555           | 2687           | 901            | 773      | 755                     | 128      | 146           | 3               | 1.05       |

**Table A2.** Gradient difference between upstream and downstream length profiles

| Fan Code | Gradient |         |            |         | Gradient Difference |
|----------|----------|---------|------------|---------|---------------------|
|          | Upstream |         | Downstream |         |                     |
|          | m per m  | Degrees | m per m    | Degrees |                     |
| A-CH-01  | 0.0185   | 1.06    | 0.0227     | 1.30    | -0.0041             |
| A-CH-02  | 0.0239   | 1.37    | 0.0192     | 1.10    | 0.0048              |
| A-CH-03  | 0.0172   | 0.99    | 0.0121     | 0.69    | 0.0052              |
| A-CH-04  | 0.0967   | 5.52    | 0.0863     | 4.93    | 0.0104              |
| A-CH-05  | 0.0593   | 3.39    | 0.0635     | 3.63    | -0.0042             |
| A-CH-06  | 0.0017   | 0.10    | 0.0008     | 0.05    | 0.0008              |
| A-CI-01  | 0.0598   | 3.42    | 0.0660     | 3.77    | -0.0061             |
| A-CI-02  | 0.1769   | 10.03   | 0.1921     | 10.88   | -0.0153             |
| A-CI-03  | 0.0489   | 2.80    | 0.0515     | 2.95    | -0.0026             |
| A-CI-04  | 0.0722   | 4.13    | 0.0866     | 4.95    | -0.0143             |
| A-CI-05  | 0.0837   | 4.78    | 0.0862     | 4.93    | -0.0025             |
| A-CO-01  | 0.0043   | 0.24    | 0.0043     | 0.24    | 0.0000              |
| A-CO-02  | 0.1995   | 11.28   | 0.2181     | 12.30   | -0.0186             |
| A-CO-03  | 0.0323   | 1.85    | 0.0208     | 1.19    | 0.0115              |
| A-CO-04  | 0.0478   | 2.74    | 0.0438     | 2.51    | 0.0040              |
| A-RO-01  | 0.1065   | 6.08    | 0.1049     | 5.99    | 0.0016              |
| A-RO-02  | 0.0260   | 1.49    | 0.0260     | 1.49    | 0.0000              |
| A-RO-03  | 0.1611   | 9.15    | 0.1633     | 9.27    | -0.0021             |
| A-SK-01  | 0.1316   | 7.50    | 0.1447     | 8.24    | -0.0132             |
| A-SK-02  | 0.1534   | 8.72    | 0.1406     | 8.00    | 0.0128              |
| A-SK-03  | 0.0739   | 4.23    | 0.0709     | 4.05    | 0.0030              |
| A-SK-04  | 0.0961   | 5.49    | 0.1237     | 7.05    | -0.0277             |
| A-ST-01  | 0.0386   | 2.21    | 0.0386     | 2.21    | 0.0000              |
| A-ST-02  | 0.0128   | 0.73    | 0.0302     | 1.73    | -0.0174             |
| A-ST-03  | 0.0367   | 2.10    | 0.0468     | 2.68    | -0.0101             |
| A-ST-04  | 0.1174   | 6.70    | 0.1161     | 6.62    | 0.0013              |
| A-ST-05  | 0.0822   | 4.70    | 0.0896     | 5.12    | -0.0074             |
| A-ST-06  | 0.1693   | 9.61    | 0.1679     | 9.53    | 0.0014              |
| A-WR-01  | 0.0766   | 4.38    | 0.0811     | 4.64    | -0.0045             |
| A-WR-02  | 0.1749   | 9.92    | 0.1759     | 9.97    | -0.0009             |
| A-WR-03  | 0.1464   | 8.33    | 0.1562     | 8.88    | -0.0098             |
| A-WR-04  | 0.1369   | 7.80    | 0.1532     | 8.71    | -0.0163             |
| Y-AL-01  | 0.0206   | 1.18    | 0.0412     | 2.36    | -0.0206             |
| Y-AL-02  | 0.0626   | 3.58    | 0.0572     | 3.28    | 0.0054              |
| Y-AL-03  | 0.0865   | 4.95    | 0.1202     | 6.85    | -0.0337             |

Table A2 (Continued)

| Fan Code | m per m | Degrees | m per m | Degrees | Gradient Difference |
|----------|---------|---------|---------|---------|---------------------|
| Y-AL-04  | 0.0641  | 3.67    | 0.0641  | 3.67    | 0.0000              |
| Y-AL-05  | 0.0556  | 3.18    | 0.0469  | 2.68    | 0.0087              |
| Y-AL-06  | 0.1200  | 6.84    | 0.1169  | 6.67    | 0.0031              |
| Y-AL-07  | 0.0034  | 0.20    | 0.0034  | 0.20    | 0.0000              |
| Y-DI-01  | 0.0984  | 5.62    | 0.1184  | 6.75    | -0.0200             |
| Y-DI-02  | 0.3006  | 16.73   | 0.2781  | 15.54   | 0.0225              |
| Y-DI-03  | 0.1350  | 7.69    | 0.1018  | 5.81    | 0.0333              |
| Y-DO-01  | 0.0270  | 1.55    | 0.0193  | 1.11    | 0.0077              |
| Y-DO-02  | 0.0624  | 3.57    | 0.0714  | 4.09    | -0.0090             |
| Y-DO-03  | 0.1986  | 11.23   | 0.2176  | 12.28   | -0.0190             |
| Y-DO-04  | 0.0073  | 0.42    | 0.0105  | 0.60    | -0.0032             |
| Y-DO-05  | 0.0257  | 1.47    | 0.0273  | 1.56    | -0.0016             |
| Y-DO-06  | 0.0145  | 0.83    | 0.0033  | 0.19    | 0.0112              |
| Y-DU-01  | 0.0571  | 3.27    | 0.0624  | 3.57    | -0.0053             |
| Y-DU-02  | 0.0221  | 1.27    | 0.0409  | 2.34    | -0.0188             |
| Y-DU-03  | 0.2034  | 11.50   | 0.1375  | 7.83    | 0.0659              |
| Y-DU-04  | 0.0586  | 3.35    | 0.0607  | 3.47    | -0.0021             |
| Y-KA-01  | 0.1269  | 7.23    | 0.1311  | 7.47    | -0.0043             |
| Y-KA-02  | 0.0762  | 4.36    | 0.0741  | 4.24    | 0.0021              |
| Y-KA-03  | 0.0807  | 4.61    | 0.0873  | 4.99    | -0.0066             |
| Y-KA-04  | 0.0239  | 1.37    | 0.0208  | 1.19    | 0.0031              |
| Y-KA-05  | 0.0708  | 4.05    | 0.0653  | 3.74    | 0.0055              |
| Y-KA-06  | 0.0950  | 5.43    | 0.0850  | 4.86    | 0.0100              |
| Y-KA-07  | 0.1159  | 6.61    | 0.0745  | 4.26    | 0.0414              |
| Y-KA-08  | 0.1556  | 8.84    | 0.1556  | 8.84    | 0.0000              |
| Y-KA-09  | 0.1573  | 8.94    | 0.1502  | 8.54    | 0.0070              |
| Y-KA-10  | 0.1611  | 9.15    | 0.1564  | 8.89    | 0.0047              |
| Y-SL-01  | 0.1206  | 6.88    | 0.1171  | 6.68    | 0.0035              |
| Y-SL-02  | 0.1495  | 8.50    | 0.1346  | 7.66    | 0.0150              |
| Y-SL-03  | 0.1199  | 6.84    | 0.1503  | 8.54    | -0.0303             |
| Y-SL-04  | 0.1377  | 7.84    | 0.1483  | 8.43    | -0.0106             |
| Y-SL-05  | 0.1051  | 6.00    | 0.1137  | 6.49    | -0.0086             |
| Y-SL-06  | 0.1316  | 7.50    | 0.1338  | 7.62    | -0.0021             |
| Y-SL-07  | 0.0162  | 0.93    | 0.0247  | 1.41    | -0.0085             |
| Y-SL-08  | 0.0501  | 2.87    | 0.0571  | 3.27    | -0.0070             |

**Table A3.** Calculated valley gradient

| Fan Code | Valley Gradient |         |
|----------|-----------------|---------|
|          | (m per m)       | Degrees |
| A-CH-01  | 0.0042          | 0.24    |
| A-CH-02  | 0.0034          | 0.19    |
| A-CH-03  | 0.0029          | 0.17    |
| A-CH-04  | 0.0029          | 0.17    |
| A-CH-05  | 0.0023          | 0.13    |
| A-CH-06  | 0.0023          | 0.13    |
| A-CI-01  | 0.0182          | 1.04    |
| A-CI-02  | 0.0182          | 1.04    |
| A-CI-03  | 0.0127          | 0.73    |
| A-CI-04  | 0.0023          | 0.13    |
| A-CI-05  | 0.0023          | 0.13    |
| A-CO-01  | 0.0012          | 0.07    |
| A-CO-02  | 0.0009          | 0.05    |
| A-CO-03  | 0.0009          | 0.05    |
| A-CO-04  | 0.0009          | 0.05    |
| A-RO-01  | 0.0043          | 0.25    |
| A-RO-02  | 0.0043          | 0.25    |
| A-RO-03  | 0.0043          | 0.25    |
| A-SK-01  | 0.0076          | 0.44    |
| A-SK-02  | 0.0076          | 0.44    |
| A-SK-03  | 0.0055          | 0.32    |
| A-SK-04  | 0.0055          | 0.32    |
| A-ST-01  | 0.0068          | 0.39    |
| A-ST-02  | 0.0068          | 0.39    |
| A-ST-03  | 0.0068          | 0.39    |
| A-ST-04  | 0.0068          | 0.39    |
| A-ST-05  | 0.0068          | 0.39    |
| A-ST-06  | 0.0068          | 0.39    |
| A-WR-01  | 0.0086          | 0.49    |
| A-WR-02  | 0.0086          | 0.49    |
| A-WR-03  | 0.0086          | 0.49    |
| A-WR-04  | 0.0086          | 0.49    |
| Y-AL-01  | 0.0026          | 0.15    |
| Y-AL-02  | 0.0016          | 0.09    |

Table A3 (Continued)

| Fan Code | Valley Gradient |         |
|----------|-----------------|---------|
|          | (m per m)       | Degrees |
| Y-AL-03  | 0.0016          | 0.09    |
| Y-AL-04  | 0.0022          | 0.13    |
| Y-AL-05  | 0.0031          | 0.18    |
| Y-AL-06  | 0.0031          | 0.18    |
| Y-AL-07  | 0.0031          | 0.18    |
| Y-DI-01  | 0.0193          | 1.11    |
| Y-DI-02  | 0.0193          | 1.11    |
| Y-DI-03  | 0.0141          | 0.81    |
| Y-DO-01  | 0.0079          | 0.45    |
| Y-DO-02  | 0.0079          | 0.45    |
| Y-DO-03  | 0.0079          | 0.45    |
| Y-DO-04  | 0.0079          | 0.45    |
| Y-DO-05  | 0.0034          | 0.19    |
| Y-DO-06  | 0.0034          | 0.19    |
| Y-DU-01  | 0.0057          | 0.33    |
| Y-DU-02  | 0.0042          | 0.24    |
| Y-DU-03  | 0.0042          | 0.24    |
| Y-DU-04  | 0.0042          | 0.24    |
| Y-KA-01  | 0.0070          | 0.40    |
| Y-KA-02  | 0.0032          | 0.18    |
| Y-KA-03  | 0.0052          | 0.30    |
| Y-KA-04  | 0.0046          | 0.26    |
| Y-KA-05  | 0.0046          | 0.26    |
| Y-KA-06  | 0.0050          | 0.29    |
| Y-KA-07  | 0.0049          | 0.28    |
| Y-KA-08  | 0.0049          | 0.28    |
| Y-KA-09  | 0.0049          | 0.28    |
| Y-KA-10  | 0.0022          | 0.13    |
| Y-SL-01  | 0.0009          | 0.05    |
| Y-SL-02  | 0.0009          | 0.05    |
| Y-SL-03  | 0.0009          | 0.05    |
| Y-SL-04  | 0.0009          | 0.05    |
| Y-SL-05  | 0.0009          | 0.05    |
| Y-SL-06  | 0.0009          | 0.05    |
| Y-SL-07  | 0.0009          | 0.05    |
| Y-SL-08  | 0.0009          | 0.05    |

